UNIVERSIDADE ESTADUAL PAULISTA
"JÚLIO DE MESQUITA FILHO"
INSTITUTO DE GEOCIÊNCIAS E CIÊNCIAS EXATAS

Trabalho de Conclusão de Curso

Curso de Graduação em Física

EXPLORATION OF THE NON-IDEAL BOSE-EINSTEIN CONDENSATION UNDER THE LIGHT OF THE GRÜNEISEN PARAMETER

Francisco Freire Barbosa

Prof. Dr. Mariano de Souza

Rio Claro (SP)

2024

UNIVERSIDADE ESTADUAL PAULISTA

Instituto de Geociências e Ciências Exatas

Câmpus de Rio Claro

FRANCISCO FREIRE BARBOSA

EXPLORATION OF THE NON-IDEAL BOSE-EINSTEIN CONDENSATION UNDER THE LIGHT OF THE GRÜNEISEN PARAMETER

Trabalho de Conclusão de Curso apresentado ao Instituto de Geociências e Ciências Exatas - Câmpus de Rio Claro, da Universidade Estadual Paulista Júlio de Mesquita Filho, para obtenção do grau de Bacharel em Física.

Rio Claro (SP)

2024

B238e

Barbosa, Francisco Freire

Exploration of the non-ideal Bose-Einstein condensation under the light of the Grüneisen parameter / Francisco Freire Barbosa. -- Rio Claro, 2024

54 p. : il., fotos

Trabalho de conclusão de curso (Bacharelado - Física) - Universidade Estadual Paulista (UNESP), Instituto de Geociências e Ciências Exatas, Rio Claro

Orientador: Mariano de Souza

Coorientador: Lucas Squillante

1. Condensação de Bose-Einstein. 2. Parâmetro de Grüneisen. 3. Interações. I. Título.

Sistema de geração automática de fichas catalográficas da Unesp. Dados fornecidos pelo autor(a).

FRANCISCO FREIRE BARBOSA

EXPLORATION OF THE NON IDEAL BOSE-EINSTEIN CONDENSATION UNDER THE LIGHT OF THE GRÜNEISEN PARAMETER

Trabalho de Conclusão de Curso apresentado ao Instituto de Geociências e Ciências Exatas - Câmpus de Rio Claro, da Universidade Estadual Paulista Júlio de Mesquita Filho, para obtenção do grau de Bacharel Física.

Comissão Examinadora

Prof. Dr. Mariano de Souza

Prof. Dr. Antonio C. Seridonio

Prof. Dr. Adriano Otuka

Rio Claro, 06 de novembro de 2024.

Assinatura da(o) aluna(o)

Assinatura da(o) orientadora(o)

ACKNOWLEDGEMENTS

I have no words to describe, what these first years of my scientific career meant to me. This was such a special period of my life which I will always remember with much love and affection. These first years would not have been so special if not for a lot of people so now I would like to acknowledge some of them. First, my advisor, Prof. Dr. Mariano de Souza, who I admire and respect so much. Professor Mariano taught me a great deal of things. Besides a lot of Physics, with him, I've learned about the true potential inherent to each person and that all of us are capable of reaching such potential. His determination, compassion, and love are true inspirations to me and I feel honored to have him as my advisor. Thank you, Professor, for all the discussions, lectures, group meetings, coffees and so on. I would like to also thank Dr. Lucas Squillante for all the support he has given me in these first years. From helping me confection the first poster for the Scientific Initiation Congress to truly heartfelt advices. It is also important to mention the imense effort of Dr. Lucas in improving the text of this B. Sc. work. His support was extremely important and for that, I am so grateful. I would like to thank my parents, Flávia Escobar Freire Barbosa and Rodrigo Amorim Barbosa. The admiration and respect I have for these two people is so profound. Thank you, Mom and Dad, for giving me such a loving life and for teaching me so much. At this point, I would like to thank my best friend and brother, Joaquim Freire Barbosa, for being a true companion and one of the most intelligent and compassionate people I know. I also thank my grandparents, Rosária Escobar Freire, Heitor Rodrigues Freire, Claudienea Amorim Barbosa, and Plínio Gonçalves Barbosa. I feel honored to be a part of this family. Finally, I want to thank my friends André Luiz Soares Jr., Gustavo Del Duque, Gustavo de Oliveira Vítor, Samuel Martignago Soares, and Lucca Sbrissa de Souza. Without these five guys, these first years would not have been so fun. I also want to thank my girlfriend Julia Onoe Gonçalves de Almeida for all the love and strength she has given me.

RESUMO

Transições de fase e fenômenos críticos podem ser explorados através de medidas do coeficiente de expansão térmica e calor específico. Neste contexto, o parâmetro de Grüneisen se mostra útil pois permite que tais fenômenos sejam explorados tanto do ponto de vista experimental como do ponto de vista teórico. Neste trabalho de conclusão de curso, é planejada a exploração de conceitos físicos associados à condensação de Bose-Einstein de partículas interagentes à luz do parâmetro de Grüneisen. Dessa forma, o objetivo deste trabalho é realizar uma análise termodinâmica de tais sistemas de modo que o efeito da interação entre partículas seja evidenciado.

Palavras-chave: Condensação de Bose-Einstein; Parâmetro de Grüneisen; Interações.

ABSTRACT

Phase transitions and critical phenomena can be explored via measurements of the thermal expansion coefficient and specific heat. In this context, the Grüneisen parameter proves itself useful because it permits that such phenomena, can be explored both theoretically and experimentally. In this B. Sc. work, the exploration of physical concepts associated with the Bose-Einstein condensation of interacting particles under the light of the Grüneisen parameter is planned. Therefore, the goal of this work is to carry out a thermodynamic analysis of such systems so that the effect of the interaction between particles becomes evident.

Keywords: Bose-Einstein condensation; Grüneisen Parameter; Interactions.

TABLE OF CONTENTS

1 INTRODUCTION 9

2 REVIEW OF THERMODYNAMICS AND STATISTICAL MECHANICS 11
2.1 Basic Thermodynamics and the Grüneisen parameter 11
2.2 Deriving the relation between c_p and c_v 13
2.3 A step-by-step deduction of the Bose-Einstein distribution . . . 15
2.4 The ideal Bose-Einstein condensation 20
2.5 Determining the critical temperature of condensation 21
2.6 Accessing the Thermodynamics of the ideal BEC 25

3 ANALYSING THE EFFECTS OF INTERACTION IN THE BOSE-EINSTEIN CONDENSATE 27
3.1 Accessing the thermodynamics of the non-ideal BEC 27
3.2 The Brillouin paramagnet and the Bose-Einstein condensation 32

4 EXPERIMENTAL ASPECTS 36
4.1 Intial discussions and predictions 36
4.2 Initial steps towards BEC experiments 37
4.3 Condensation of alkali diluted gases 38
4.4 The Solid State Physics Laboratory 40

5 EXPLORING THE THERMODYNAMICS OF THE NON-IDEAL BEC 43
5.1 Volume and pressure parameters for harmonically trapped particles 43
5.2 Computing the Grüneisen ratio 47

6 CONCLUSIONS AND PERSPECTIVES 51

BIBLIOGRAPHY 52

1 INTRODUCTION

The Bose-Einstein condensation (BEC) consists of a macroscopic occupation of the ground state of a system composed of bosons as the temperature $T \to 0$ [5]. This phenomenon was originally predicted in the beginning of the last century by A. Einstein and S. Bose in a series of seminal papers [6, 7] while its first experimental realization was achieved in 1995 through the use of harmonic trapped particles [8, 9]. The initial predictions of the BEC concerned exclusively non-interacting particles, so that the effects of interaction became a topic of discussion in the community. Hence, the goal of this B. Sc. work, is to explore the interacting BEC under the light of the so-called Grüneisen parameter, which has already been extensively employed in the analysis of a myriad of phase transitions and critical phenomena [10–12]. Hence, this B. Sc. work is divided in the following manner:

- **Chapter 2**: This chapter presents a review of basic Thermodynamics based on Ref. [13]. We shall revisit important quantities like the specific heat, the compressibility, and the thermal expansion coefficient. Furthermore, we introduce the Grüneisen parameter and discuss its applications in the analysis of phase transitions and critical phenomena. At the end of this section, a relation between the specific heats is derived. Such a relation will be important in the thermodynamic analysis of the BEC in Chapter 5. Furthermore, in this chapter, the framework of the ideal Bose gas and the ideal BEC is reviewed. We begin by deriving the Bose-Einstein distribution in a step-by-step fashion, following the deduction presented in Ref. [14]. In the following, we discuss the ideal BEC and present a few of its thermodynamic properties cf. Ref. [5].

- **Chapter 3**: In this Chapter, the framework of the non-ideal BEC is presented following Refs. [14, 15]. We shall evaluate the eigenenergies of a Hamiltonian which describes a system of weakly interacting bosons and discuss the effects of interactions in such systems. Furthermore, we discuss the non-ideal BEC in analogy with the Brillouin paramagnet, following results reported in Ref. [11].

- **Chapter 4**: In this part of the text we review historical and experimental aspects concerning the initial predictions and experiments involving the BEC. Although we are not able to perform the BEC, the experiments conducted by Prof. Dr. Mariano de Souza in the Solid State Physics lab supplement all the theoretical results obtained by the group. With that in mind, we shall cover important aspects concerning the thermal expansion measurements performed at the lab.

- **Chapter 5**: In this chapter a thermodynamic analysis of the non-ideal harmonic trapped BEC is presented. To do so, we revisit the recently defined volume and pressure parameters which emulate the conventional quantities known as volume and pressure [16]. Through the analysis of experimental data concerning such parameters, we will be able to compute the Grüneisen ratio for such systems and analyze its behavior in the vicinity of the critical temperature.

- **Chapter 6-7**: Conclusions and perspectives are presented. We shall briefly review all that was discussed in this B. Sc. work. In chapter 7, we acknowledge the people who made this B. Sc. work possible.

2 REVIEW OF THERMODYNAMICS AND STATISTICAL MECHANICS

In this chapter, a review of Thermodynamics and Statistical Mechanics is presented. We shall start with a discussion concerning the Grüneisen parameter along with thermodynamic considerations about phase transitions and critical phenomena. In the following, a step-by-step derivation of the Bose-Einstein distribution is presented. The remainder of this chapter focuses on the ideal BEC.

2.1 BASIC THERMODYNAMICS AND THE GRÜNEISEN PARAMETER

The interplay between the thermodynamic quantities of the system is a pivotal point in the description of phase transitions and critical phenomena. Hence, following the steps of Stanley's seminal book [13], we revisit some important quantities in Thermodynamics, which tell us how certain properties of the system change with respect to external stimuli. First, we have the specific heat, which tells us how the temperature T changes as heat is added or removed from the system [17]. The specific heat at constant volume v, is expressed by:

$$c_v = T\left(\frac{\partial S}{\partial T}\right)_v = \left(\frac{\partial U}{\partial T}\right)_v = -T\left(\frac{\partial^2 F}{\partial T^2}\right)_v, \tag{2.1}$$

where S is the entropy, U the internal energy, and F the Helmholtz free energy. The index v indicates that such a process is occurring for constant values of volume. In the same manner, we can write the specific heat at constant pressure as:

$$c_p = T\left(\frac{\partial S}{\partial T}\right)_p = \left(\frac{\partial H}{\partial T}\right)_p = -T\left(\frac{\partial^2 G}{\partial T^2}\right)_p, \tag{2.2}$$

where p is the pressure, H is the enthalpy, and G the Gibbs free energy. We can also define expressions for the system's compressibility, a function that quantifies variations of v with respect to p, which can be under constant temperature or entropy. For the isothermal case, we have:

$$\kappa_T = -\frac{1}{v}\left(\frac{\partial v}{\partial p}\right)_T = \frac{1}{\rho}\left(\frac{\partial \rho}{\partial p}\right)_T = -\frac{1}{v}\left(\frac{\partial^2 G}{\partial p^2}\right)_T, \tag{2.3}$$

where ρ is density, while for the adiabatic case:

$$\kappa_S = -\frac{1}{v}\left(\frac{\partial v}{\partial p}\right)_S = \frac{1}{\rho}\left(\frac{\partial \rho}{\partial p}\right)_S = -\frac{1}{v}\left(\frac{\partial^2 E}{\partial p^2}\right)_S. \tag{2.4}$$

Last but not least, we have the thermal expansion coefficient, defined as:

$$\alpha_p = \frac{1}{v_0}\left(\frac{\partial v}{\partial T}\right)_p = -\frac{1}{v_0}\left(\frac{\partial S}{\partial p}\right)_T. \tag{2.5}$$

The functions previously defined are so important because they tell us how the physical properties of the system evolve with variations of temperature, pressure, and density

and thus, how they behave when going through phase transitions or in the vicinity of critical points. Under such conditions, these functions will behave in a specific manner, presenting divergences, and changes of sign due to the exotic character of such critical conditions [13]. Hence, the analysis of quantities like c_p, κ_T, and α_p enables us not only to study the Physics of phase transitions and critical points but also to identify such phenomena in situations when very little is known about the system. In this context, the so-called effective Grüneisen parameter Γ_{eff} [18], is defined as:

$$\Gamma_{eff} = \frac{v\alpha_p}{\kappa_T c_v}. \tag{2.6}$$

Such parameter proved itself to be very useful in the analysis of phase transitions and critical phenomena. Due to the fact that Γ_{eff} incorporates quantities like α_p, c_v, and κ_T, it becomes clear that such parameter holds much information about the physical systems in question. Γ_{eff} has already been employed in the analysis of such phenomena, presenting very unique behavior such as changes of sign where going through phase transitions and divergent behaviors near critical points. It was proposed that Γ_{eff} can be written in terms of the ratio $\frac{\alpha_p}{c_p}$ if we simply multiply the right side of Eq. 2.6 by $\frac{c_p}{c_p}$ [19]. Thus we have:

$$\Gamma_{eff} = \frac{v\alpha_p}{K_T c_v}\frac{c_p}{c_p} = \frac{\alpha_p}{c_p}\frac{vc_p}{K_T c_v}. \tag{2.7}$$

The ratio between α_p and c_p is denoted by Γ and is known as the Grüneisen ratio. Additionally, it was proposed that this ratio is the singular part of Γ_{eff}, i.e., the part responsible for the divergent behaviors near critical points [19]. This is due to the fact that α_p which is present in the definition of Γ is extremely sensitive to variation of S. We will discuss in detail the physical origin of this singular behavior of α_p in the last chapter, in which we analyze the Thermodynamics of the BEC. The Grüneisen ratio can be expressed in various ways by manipulating the thermodynamic relations we already defined. Hence we can write Γ as:

$$\Gamma = \frac{\alpha_p}{c_p} = \frac{1}{v_0}\left(\frac{\partial v}{\partial T}\right)_p \left[\frac{1}{\frac{T}{N}\left(\frac{\partial S}{\partial T}\right)_p}\right] = \frac{1}{v_m T}\left(\frac{\partial v}{\partial T}\right)_p, \tag{2.8}$$

where v_m is the so-called molar volume. Note that v_m appears in this context because we simply divided the expression for c_p in terms of the entropy by the total number of particles N. This quantity is referred to as the molar specific heat [13]. We can also rewrite the entropy derivatives in the numerator and in the denominator of Eq. 2.8 in the following way:

$$\left(\frac{\partial S}{\partial p}\right)_T = -\frac{\partial}{\partial p}\left(\frac{\partial G}{\partial T}\right) = -\left(\frac{\partial^2 G}{\partial p \partial T}\right), \tag{2.9}$$

$$\left(\frac{\partial S}{\partial T}\right)_p = -\frac{\partial}{\partial T}\left(\frac{\partial G}{\partial T}\right) = -\left(\frac{\partial^2 G}{\partial T^2}\right). \tag{2.10}$$

Thus, Γ becomes:

$$\Gamma = -\frac{1}{Tv_m}\frac{\left(\frac{\partial^2 G}{\partial p \partial T}\right)}{\left(\frac{\partial^2 G}{\partial T^2}\right)}. \tag{2.11}$$

By rewriting the derivatives we can see clearly the dependence of Γ on the tuning parameters, which in this case are temperature and pressure. Furthermore, we can make use of the thermodynamic relation [13]:

$$\left(\frac{\partial S}{\partial T}\right)_p \left(\frac{\partial T}{\partial p}\right)_S \left(\frac{\partial p}{\partial S}\right)_T = -1, \tag{2.12}$$

which we can solve for $\left(\frac{\partial T}{\partial p}\right)_S$:

$$\left(\frac{\partial T}{\partial p}\right)_S = \frac{-1}{\left(\frac{\partial S}{\partial T}\right)_p \left(\frac{\partial p}{\partial S}\right)_T} = -\frac{\left(\frac{\partial S}{\partial p}\right)_T}{\left(\frac{\partial S}{\partial T}\right)_p}, \tag{2.13}$$

and substituting in Eq. 2.8 we achive:

$$\Gamma = \frac{1}{Tv_m}\left(\frac{\partial T}{\partial p}\right)_S. \tag{2.14}$$

Note that the expression above quantifies adiabatic temperature changes with respect to pressure, such phenomena are known as caloric effects. More specifically, Eq. 2.14 refers to the barocaloric effect because the temperature adiabatically changes by tuning pressure. A more general definition of Γ would be:

$$\Gamma = \frac{1}{T}\left(\frac{\partial T}{\partial g}\right)_S, \tag{2.15}$$

where g is a tuning parameter such as magnetic and electric fields and stress, each one being associated with a corresponding caloric effect [20].

2.2 DERIVING THE RELATION BETWEEN c_p AND c_v

Following the last section's discussion on Thermodynamics based on Stanley's book [13], we shall derive a relation between c_p and c_v that will be useful in the thermodynamic analysis of the BEC, presented in the last chapter. Let us start by writing the difference $c_p - c_v$ in terms of S and multiply this by κ_T. Thus, we have:

$$\kappa_T(c_p - c_v) = -\frac{1}{v}\left(\frac{\partial v}{\partial p}\right)_T \left[T\left(\frac{\partial S}{\partial T}\right)_p - T\left(\frac{\partial S}{\partial T}\right)_v\right]. \tag{2.16}$$

Recalling the thermodynamic relation:

$$\left(\frac{\partial S}{\partial T}\right)_p = \left(\frac{\partial S}{\partial T}\right)_v + \left(\frac{\partial S}{\partial v}\right)_T \left(\frac{\partial v}{\partial T}\right)_p, \tag{2.17}$$

which we can substitute in Eq. 2.16 and thus obtain:

$$\kappa_T(c_p - c_v) = -\frac{T}{v}\left(\frac{\partial v}{\partial p}\right)_T \left[\cancel{\left(\frac{\partial S}{\partial T}\right)_v} + \left(\frac{\partial S}{\partial v}\right)_T \left(\frac{\partial v}{\partial T}\right)_p - \cancel{\left(\frac{\partial S}{\partial T}\right)_v}\right], \tag{2.18}$$

$$\kappa_T(c_p - c_v) = -\frac{T}{v}\left(\frac{\partial v}{\partial p}\right)_T \left(\frac{\partial S}{\partial v}\right)_T \left(\frac{\partial v}{\partial T}\right)_p. \tag{2.19}$$

The product of the three partial derivatives can be simplified if we recall:

$$\left(\frac{\partial v}{\partial p}\right)_T \left(\frac{\partial p}{\partial T}\right)_v \left(\frac{\partial T}{\partial v}\right)_p = -1, \tag{2.20}$$

so that:

$$\left(\frac{\partial v}{\partial p}\right)_T \left(\frac{\partial p}{\partial T}\right)_v = -\left(\frac{\partial v}{\partial T}\right)_p. \tag{2.21}$$

Through the Maxwell relation $\left(\frac{\partial p}{\partial T}\right)_v = \left(\frac{\partial S}{\partial v}\right)_T$., we can rewrite Eq. 2.21 as:

$$\left(\frac{\partial v}{\partial p}\right)_T \left(\frac{\partial p}{\partial T}\right)_v = -\left(\frac{\partial v}{\partial T}\right)_p. \tag{2.22}$$

Substituting the expression above in Eq. 2.19, we achive:

$$\kappa_T(c_p - c_v) = \frac{T}{v}\left(\frac{\partial v}{\partial p}\right)_T^2 \left(\frac{\partial p}{\partial T}\right)_v^2. \tag{2.23}$$

By writting κ_T according to its deffinition in Eq. 2.3:

$$-\frac{1}{\cancel{v}}\cancel{\left(\frac{\partial v}{\partial p}\right)_T}(c_p - c_v) = \frac{T}{\cancel{v}}\left(\frac{\partial v}{\partial p}\right)_T^{\cancel{2}} \left(\frac{\partial p}{\partial T}\right)_v^2, \tag{2.24}$$

$$-(c_p - c_v) = c_v - c_p = T\left(\frac{\partial v}{\partial p}\right)_T \left(\frac{\partial p}{\partial T}\right)_v^2. \tag{2.25}$$

Hence, we finally achive the relation:

$$\boxed{c_p = c_v - T\frac{\left(\frac{\partial p}{\partial T}\right)_v^2}{\left(\frac{\partial p}{\partial v}\right)_T}.} \tag{2.26}$$

We can apply such relation to the ideal gas law, namely $pv = nRT$, where R is the ideal gas universal constant [17]. By evaluating the derivatives we get:

$$\left(\frac{\partial p}{\partial T}\right)_v^2 = \frac{N^2R^2}{v^2}; \quad \left(\frac{\partial p}{\partial v}\right)_T = -\frac{NRT}{v^2}. \tag{2.27}$$

By substituting the expressions above in the relation we derived, we achieve that the relation between c_p and c_v for the ideal gas is simply:

$$c_p - c_v = NR. \tag{2.28}$$

2.3 A STEP-BY-STEP DEDUCTION OF THE BOSE-EINSTEIN DISTRIBUTION

In the microscopic world, particles can be separated into two groups which essentially differ from each other by the value of their spin [21]. If a particle has a value of spin that is an integer multiple of Planck's constant h, it is said to be a boson. On the other hand, if the particle's spin is a half-integer multiple of h, then the particle is a fermion [22]. Curiously, according to Pauli's exclusion principle, fermions are not allowed to occupy the same quantum state, while bosons are able to do so. Such a feature of bosonic particles will play a key role in the BEC [23]. In this section, a step-by-step deduction of the Bose-Einstein distribution is presented following the steps of Pathria's book on Statistical Mechanics [14]. Such distribution displays the expected occupancy of bosons $\langle n_\alpha \rangle$ in a certain energy level α while the analogous one for fermions is known as the Fermi-Dirac distribution which is not contemplated in this text. The two distribution functions mentioned refer to quantum gases while classical gases obey the Boltzmann distribution. In Fig. 1, we can see a comparison between such distributions as a function of $(\varepsilon_\alpha - \mu)/k_B T$ where ε_α is the energy of level α, μ is the chemical potential and k_B Boltzmann's constant. It is possible for multiple states to be associated with the same energy value, these are the so-called degenerate energy levels [14]. The number of states associated to a single level is called degeneracy and is denoted by g_α. To start the demonstration, we consider a system with N indistinguishable bosonic particles distributed in a number α of energy levels, with each level being associated with the value of energy ε_α. We can express the total number of particles and the total energy of the system as:

$$N = \sum_\alpha n_\alpha, \tag{2.29}$$

$$U = \sum_\alpha n_\alpha \varepsilon_\alpha, \tag{2.30}$$

where n_α is the number of particles per level α. In the context of statistical analysis, a key quantity to be defined is the system's multiplicity $\Omega(N, v, E)$, which provides us with the number of microstates associated to one macrostate. Hence, in the context of occupation numbers in Statistical Mechanics, the system's multiplicity Ω is the number of different configurations of N particles distributed in all of the α energy levels. Thus we can write:

$$\Omega(N, v, E) = \sum_\alpha W\left\{n_\alpha\right\}, \tag{2.31}$$

where $W\left\{n_\alpha\right\}$ is the number of possible microstates associated to a distribution $\{n_\alpha\}$. To access $W\left\{n_\alpha\right\}$ we must compute all the different manners in which n_α particles can be distributed in the g_α states, which we shall denote by $w(\alpha)$.

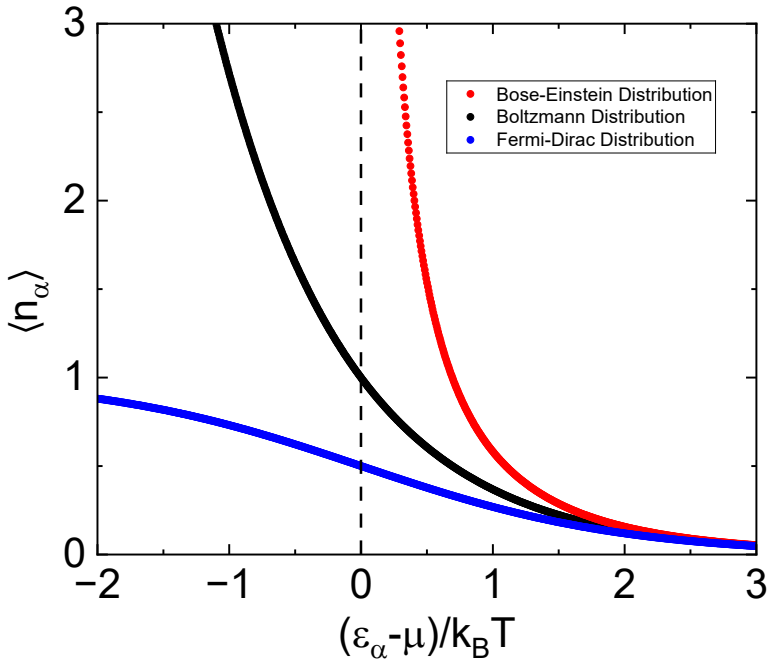


Figure 1 – The three distribution functions of Statistical Mechanics, namely, the Bose-Einstein, Boltzmann, and Fermi-Dirac. Note that for $(\varepsilon_\alpha - \mu)/k_BT = 0$ the Bose-Einstein distribution diverges, which is a manifestation of the condensation. Figure adapted from Ref. [14]

.

Since we are dealing with bosons, which are indistinguishable, $w(\alpha)$ is given by [14]:

$$w\left\{n_\alpha\right\} = \frac{(n_\alpha + g_\alpha - 1)!}{n_\alpha!(g_\alpha - 1)!}. \tag{2.32}$$

Therefore, $W\left\{n_\alpha\right\}$ can be written as the product:

$$W\left\{n_\alpha\right\} = \prod_\alpha w(\alpha), \tag{2.33}$$

which embodies all the distributions of n_α particles in g_α states. With multiplicity in hands, it becomes possible to achieve an expression for the system's entropy, following the definition of Boltzmann's entropy:

$$S = k_B \ln \Omega. \tag{2.34}$$

Thus we have:

$$S = k_B \ln \left[\sum_{n_\alpha} W\left\{n_\alpha\right\}\right]. \tag{2.35}$$

Since we are looking for the expression that yields the most probable distribution of particles we should analyze the system in the most probable scenario. According to the second law of Thermodynamics, this is the equilibrium situation in which the entropy is

maximized. Hence, we should look for the distribution set $\{n_\alpha^*\}$ which maximizes S. With that in mind, we can neglect the less probable distributions sets the sum in Eq. 2.35. Thus we have:

$$S \approx k_B \ln W\{n_\alpha^*\}, \tag{2.36}$$

This maximization of the entropy occurs under the conditions that the energy E and the number of particles N remain constant. Mathematically, we can go through such a process of maximization by making use of the Lagrange multipliers method. Such a method consists of determining the maximum of a function $f(x)$ under a certain constraint $g(x)$ [24]. To do so, we compute the derivative of $f(x)$ with respect to $g(x)$ and set it to zero. The constraints are imposed by a number which is multiplied by the differential of $g(x)$ [25]. The general form, of a maximization occurring through the Lagrange multipliers with two constraints $g(x)$ and $h(x)$ is:

$$\delta f(x,y) - \eta \times \delta g(x,y) - \beta \times \delta h(x,y) = 0, \tag{2.37}$$

where δ represents an infinitesimal increment in the functions and η and β are the multipliers. In this context, constraints are Eqs. 2.29 and 2.30. This means that we are looking for the maximum value of S under these specific conditions. If the values of E and N were arbitrary, there would be infinite microstates and thus infinite entropy. Thus we have:

$$\delta \ln W\{n_\alpha\} - \left[\eta \sum_\alpha \delta n_\alpha + \beta \sum_\alpha \varepsilon_\alpha \delta n_\alpha\right] = 0. \tag{2.38}$$

Recalling that $W\{n_\alpha\}$ contains a product over the α levels in its definition we can rewrite it by using the basic property of logarithms $\log(a \times b) = \log(a) + \log(b)$. So the first term in the equation above becomes:

$$\ln W\{n_\alpha\} = \ln \prod_\alpha w(\alpha) = \sum_\alpha \ln w(\alpha), \tag{2.39}$$

$$\sum_\alpha \ln w(\alpha) = \sum_\alpha \{\ln(n_\alpha + g_\alpha - 1)! - \ln[n_\alpha!(g_\alpha - 1)!]\}. \tag{2.40}$$

Recalling Stirling's approximation, $\ln x! = x \ln x - x$, which can be applied in this context if n_α and g_α are both $>> 1$ [14], we have:

$$\begin{aligned}\sum_\alpha \ln w(\alpha) = \sum_\alpha \{&[(n_\alpha + g_\alpha - 1)\ln(n_\alpha + g_\alpha - 1)] \\ &\cancel{-n_\alpha - g_\alpha + 1} - [n_\alpha \ln(n_\alpha)] + \cancel{n_\alpha} - [(g_\alpha - 1)\ln(g_\alpha - 1)] + \cancel{g_\alpha - 1}\}.\end{aligned} \tag{2.41}$$

Eliminating the crossed-out terms we have:

$$\begin{aligned}\sum_\alpha \ln w(\alpha) = \sum_\alpha \{&[(n_\alpha + g_\alpha - 1)\ln(n_\alpha + g_\alpha - 1)] \\ &-n_\alpha \ln n_\alpha - (g_\alpha - 1)\ln(g_\alpha - 1)\}.\end{aligned} \tag{2.42}$$

We can further simplify this because we have assumed that both n_α and g_α are both $>> 1$, so we are left with:

$$\sum_\alpha \ln w(\alpha) = \sum_\alpha \{(n_\alpha + g_\alpha)\ln(n_\alpha + g_\alpha) - n_\alpha \ln n_\alpha - g_\alpha \ln g_\alpha\}, \tag{2.43}$$

$$= \sum_\alpha \{n_\alpha \ln(n_\alpha + g_\alpha) + g_\alpha \ln(n_\alpha + g_\alpha) - n_\alpha \ln n_\alpha - g_\alpha \ln g_\alpha\}. \tag{2.44}$$

By grouping the terms multiplied by n_α and g_α we have:

$$\sum_\alpha \ln w(\alpha) = \sum_\alpha \{n_\alpha[\ln(n_\alpha + g_\alpha) - \ln n_\alpha] + g_\alpha[\ln(n_\alpha + g_\alpha) - \ln g_\alpha]\}, \tag{2.45}$$

in a way that:

$$\sum_\alpha \ln w(\alpha) = \sum_\alpha \left[n_\alpha \ln\left(\frac{g_\alpha}{n_\alpha} + 1\right) + g_\alpha \ln\left(\frac{n_\alpha}{g_\alpha} + 1\right)\right] = \ln W\{n_\alpha\}. \tag{2.46}$$

It is important to remember that all these steps are needed in order to write an expression for $\ln W\{n_\alpha\}$. The first term in Eq. 2.38 is simply the derivative of $\ln W\{n_\alpha\}$ with respect to n_α. Thus, we can differentiate the expression in Eq. 2.46 with respect to n_α and replace the final expression in Eq. 2.38. By applying the chain and product rules, we have:

$$\frac{\delta \ln W\{n_\alpha\}}{\delta n_\alpha} = \sum_\alpha \left[\ln\left(\frac{g_\alpha}{n_\alpha} + 1\right) - n_\alpha \frac{1}{\left(1 + \frac{g_\alpha}{n_\alpha}\right)} \frac{g_\alpha}{n_\alpha^2} + \frac{g_\alpha}{\left(\frac{n_\alpha}{g_\alpha} + 1\right)} \frac{1}{g_\alpha}\right], \tag{2.47}$$

$$\frac{\delta \ln W\{n_\alpha\}}{\delta n_\alpha} = \sum_\alpha \left[\ln\left(\frac{g_\alpha}{n_\alpha} + 1\right) - \frac{\cancel{g_\alpha}}{\cancel{n_\alpha} + g_\alpha} + \frac{\cancel{g}}{\cancel{n_\alpha} + g_\alpha}\right], \tag{2.48}$$

$$\frac{\delta \ln W\{n_\alpha\}}{\delta n_\alpha} = \sum_\alpha \ln\left(\frac{g_\alpha}{n_\alpha} + 1\right), \tag{2.49}$$

$$\delta \ln W\{n_\alpha\} = \sum_\alpha \ln\left(\frac{g_\alpha}{n_\alpha} + 1\right)\delta n_\alpha. \tag{2.50}$$

By plugging Eq. 2.50 into Eq. 2.38 we achive:

$$\sum_\alpha \ln\left(\frac{g_\alpha}{n_\alpha} + 1\right)\delta n_\alpha - \left[\eta \sum_\alpha \delta n_\alpha + \beta \sum_\alpha \varepsilon_\alpha \delta n_\alpha\right] = 0, \tag{2.51}$$

$$\sum_\alpha \left[\ln\left(\frac{g_\alpha}{n_\alpha} + 1\right) - \eta - \beta\varepsilon_\alpha\right]\delta n_\alpha = 0. \tag{2.52}$$

Recalling that we are determining the distribution set $\{n_\alpha^*\}$ which maximizes the entropy. Hence, the denominator inside the logarithm reffers specifically to the distribution n_α that corresponds to the equilibrium situation, i.e., the most probable one. In order to emphasize this point, we shall denote such distribution as n_α^*. So we achieve:

$$\sum_\alpha \left[\ln\left(\frac{g_\alpha}{n_\alpha^*} + 1\right) - \eta - \beta\varepsilon_\alpha\right]\delta n_\alpha = 0. \tag{2.53}$$

We know for a fact the increment δn_α is different from zero so the only way for the equality above to be true is if:

$$\ln\left(\frac{g_\alpha}{n^*_\alpha}+1\right)-\eta-\beta\varepsilon_\alpha=0. \tag{2.54}$$

Before proceeding we shall discuss the physical meaning of the Lagrange multipliers η and β. As we have already discussed, the multipliers are responsible for ensuring the constraints that N and E remain constant. Hence, η imposes that we are in fact looking for the most probable distribution for a certain finite N and not for any value of N. This is imposed with we multiply this distribution n^*_α for its associated chemical potential μ but weighted by $1/k_BT$. That is because μ/k_BT ensures that we are distributing a finite number of particles along the α levels. With that in mind, we can see that η can be expressed as μ/k_BT. In a similar manner, β ensures that the energy associated with the most probable distribution is finite and not arbitrary. The total energy of this system at a given T is k_BT so β can be expressed as $1/k_BT$. Substituting η and β we have [14]:

$$\eta=-\frac{\mu}{k_BT};\quad \beta=\frac{1}{k_BT}. \tag{2.55}$$

Hence, we have that the expression for n^*_α is:

$$n^*_\alpha=\frac{g_\alpha}{e^{(\varepsilon_\alpha-\mu)/k_BT}-1}. \tag{2.56}$$

This expression gives us the most probable value of the number of particles in a determined level α. We aim to show now that the most probable value of n_α is exactly equal to its mean value $\langle n_\alpha\rangle$. To do so we recall the relation:

$$\langle n_\alpha\rangle=-k_BT\left(\frac{\partial q}{\partial\varepsilon_\alpha}\right), \tag{2.57}$$

where the quantity q is the logarithm of the system's grand partition function $\mathcal{L}$, which is given by:

$$\mathcal{L}=\prod_{\varepsilon_\alpha}\frac{1}{[1-ze^{-(\varepsilon_\alpha/k_BT)}]}, \tag{2.58}$$

where z is the system's fugacity, given by $z=e^{(\mu/k_BT)}$ [14]. Hence, we can write q as:

$$q=-\sum_{\varepsilon_\alpha}\ln\left(1-ze^{-(\varepsilon_\alpha/k_BT)}\right). \tag{2.59}$$

Evaluating the derivative of q with respect to ε_α we have that:

$$\frac{\partial q}{\partial\varepsilon_\alpha}=-\frac{\partial}{\partial\varepsilon_\alpha}\ln\left(1-ze^{-(\varepsilon_\alpha/k_BT)}\right). \tag{2.60}$$

Note that the summation disappears because we are differentiating q with respect to a single value of ε, namely, ε_α. Since the summation runs over all values of ε, these other values do not contribute to the derivative. Hence:

$$\frac{\partial}{\partial\varepsilon_\alpha}\ln\left(1-ze^{-(\varepsilon_\alpha/k_BT)}\right)=\frac{1}{1-ze^{-(\varepsilon_\alpha/k_BT)}}\left(-\frac{\partial}{\partial\varepsilon_\alpha}\left(1-ze^{-(\varepsilon_\alpha/k_BT)}\right)\right). \tag{2.61}$$

The derivative on the right-hand side is:

$$\frac{\partial}{\partial \varepsilon_\alpha}\left(1 - ze^{-(\varepsilon_\alpha/k_BT)}\right) = ze^{-(\varepsilon_\alpha/k_BT)}\left(-\frac{1}{k_BT}\right). \tag{2.62}$$

Thus we achieve the result:

$$\frac{\partial}{\partial \varepsilon_\alpha}\ln\left(1 - ze^{-(\varepsilon_\alpha/k_BT)}\right) = \frac{ze^{-(\varepsilon_\alpha/k_BT)}}{\left(1 - ze^{-(\varepsilon_\alpha/k_BT)}\right)}\left(-\frac{1}{k_BT}\right), \tag{2.63}$$

which can be replaced in Eq. 2.57 so we have:

$$\langle n_\alpha\rangle = -\cancel{k_BT}\left(\frac{-1}{\cancel{k_BT}}\frac{ze^{-(\varepsilon_\alpha/k_BT)}}{1 - ze^{-(\varepsilon_\alpha/k_BT)}}\right). \tag{2.64}$$

$$\langle n_\alpha\rangle = \frac{ze^{-(\varepsilon_\alpha/k_BT)}}{1 - ze^{-(\varepsilon_\alpha/k_BT)}}. \tag{2.65}$$

Multiplying the expression above by $\frac{ze^{(\varepsilon_\alpha/k_BT)}}{ze^{(\varepsilon_\alpha/k_BT)}}$ and replacing z by its definition, we achive:

$$\langle n_\alpha\rangle = \frac{1}{e^{(\varepsilon_\alpha-\mu)/k_BT} - 1}. \tag{2.66}$$

Note that n^*_α is identical to $\langle n_\alpha\rangle$ for $g_\alpha = 1$, so we finally achieve:

$$\boxed{n^*_\alpha = \langle n_\alpha\rangle = \frac{1}{e^{(\varepsilon_\alpha-\mu)/k_BT} - 1},} \tag{2.67}$$

which is the expression for the Bose-Einstein distribution [14].

2.4 THE IDEAL BOSE-EINSTEIN CONDENSATION

When dealing with bosons at temperatures near the limit $T \to 0$, the phenomena known as BEC occurs [6]. It consists of all the system's particles occupying the ground state and hence being governed by the same wave function. Due to the fact that the particles in question are bosons and not fermions, they are allowed to occupy the same state according to Pauli's exclusion principle [14]. Following the discussions in Ralph Baierlein's book Thermal Physics [5], the theoretical framework of the ideal BEC will be revisited. The expected value of the number of particles for each level α is:

$$\langle n_\alpha\rangle = \frac{1}{e^{(\varepsilon_\alpha-\mu)/k_BT} - 1}. \tag{2.68}$$

The total number of particles in the system can be written as a sum of the expected values of n for each state α:

$$N = \sum_\alpha \langle n_\alpha\rangle, \tag{2.69}$$

As it was mentioned, in the condensation threshold, i.e., $T \to 0$, all the particles will occupy the lowest energy state. By denoting such state as α= 1, we can write:

$$N = \lim_{T\to 0}\langle n_1\rangle = \lim_{T\to 0}\frac{1}{e^{(\varepsilon_1-\mu)/k_BT} - 1}. \tag{2.70}$$

Hence it becomes possible to infer how the chemical potential will behave in such a limit. Knowing that $\langle n_1 \rangle$ is a positive finite number and that N is a large one, we can assume not only that $\mu < \varepsilon_1$ but also that both these quantities have a very close value since N is large. By expanding the exponential in Eq. 2.70 as a Taylor series [24]:

$$e^x = 1 + x + \frac{x^2}{2!} + \frac{x^3}{3!}..., \tag{2.71}$$

we have:

$$N = \frac{1}{1 + (\varepsilon_1 - \mu)/k_B T + ... - 1}, \tag{2.72}$$

since the higher power terms of the series will be so small, we can neglect them and thus:

$$N = \frac{1}{1 + (\varepsilon_1 - \mu)/k_B T - 1} = \frac{k_B T}{\varepsilon_1 - \mu}. \tag{2.73}$$

Solving for the chemical potential we can see that:

$$\mu = \varepsilon_1 - \frac{k_B T}{N}, \tag{2.74}$$

and by taking the limit $T \to 0$:

$$\mu = \varepsilon_1. \tag{2.75}$$

In summary, for $T \to 0$ the chemical potential has the same value as the lowest energy level. The physical interpretation behind this equality is the following: since $T \to 0$, it becomes clear that $E = k_B T \to 0$, hence the system is free of any thermal energy to excite the particles to higher energy levels and so they settle in the ground state. Since the only available level is the lowest one, the chemical potential of the entire system becomes solely the energy of the ground state and thus we conclude that $\mu = \varepsilon_1$.

2.5 DETERMINING THE CRITICAL TEMPERATURE OF CONDENSATION

A question that arises once the condensation threshold is properly analyzed is: what exactly is the temperature at which the condensation starts to happen? To answer this question we must fully comprehend the interplay between quantities like temperature, energy, and chemical potential. As we have seen before, cf. $T \to 0$ we have that $\mu \to \varepsilon_1$. That's the major requirement for the condensation to happen. On the other hand, if we increase the temperature the chemical potential will decrease until zero and remain negative for all values of $T > T_c$ [14]. We can see that μ is zero at $T = T_c$ through a careful analysis of Eq. 2.74. Due to the fact that we are dealing with an ideal Bose gas, the only energy scale present is the thermal one in a way that the second term in Eq. 2.74 represents the total energy per particle. With that in mind, we can interpret T_c as the temperature at which the thermal energy per particle becomes $\leqslant \varepsilon_1$. Hence, it becomes clear that for $T = T_c$, $k_B T_c/N = \varepsilon_1$ and thus $\mu = 0$. As a consequence, for $T \geqslant T_c$, the thermal energy per particle is $k_B T \geqslant \varepsilon_1$, and thus no particles occupy the ground state.

Hence if we evaluate the system in the condition that $\mu = 0$, we may find an expression for the critical temperature, i.e., the temperature at which the condensation starts to take place. With this goal in mind we first rewrite Eq. 2.69, replacing the sum over all the possible levels with an integral that goes over all the available energies. We integrate the product between the expected number of particles $\langle n_\alpha \rangle$ and the density of states $D(\varepsilon)$, defined as [5]:

$$D(\varepsilon) = \frac{2\pi(2m)^{3/2}}{h^3} v\varepsilon^{1/2}, \tag{2.76}$$

where m is the particle's mass. This quantity provides the total number of accessible states in a determined energy range [5]. Hence, N can be computed as:

$$N = \int_0^\infty \langle n_\alpha \rangle D(\varepsilon) d\varepsilon, \tag{2.77}$$

$$N = \int_0^\infty \frac{1}{e^{(\varepsilon-\mu)/k_B T} - 1} D(\varepsilon) d\varepsilon. \tag{2.78}$$

Note that we have dropped the subscript α, that is because we are now integrating over a continuous spectrum of energy, rather than evaluating a sum over discreet α energy levels. Since we are dealing with the limit where the condensation starts to happen, we consider a critical temperature T_c that makes $\mu = 0$. Thus, by solving the integral we get the number of particles in the excited states, which in this case is the total number of particles in the system:

$$N = \int_0^\infty \frac{1}{e^{(\varepsilon/k_B T_c)} - 1} D(\varepsilon) d\varepsilon. \tag{2.79}$$

We can write $D(\varepsilon) = C\varepsilon^{1/2}$ where C represents the constants in the definition of the density of states [5]. Hence:

$$N = \int_0^\infty \frac{C\varepsilon^{1/2}}{e^{\varepsilon_\alpha/k_B T_c} - 1} d\varepsilon, \tag{2.80}$$

making the substitution $x = \varepsilon/k_B T_c$ we have:

$$N = C(k_B T_c)^{3/2} \int_0^\infty \frac{x^{1/2}}{e^x - 1} d\varepsilon, \tag{2.81}$$

which is a tabulated integral [24] present in the definition of the Zeta function $\zeta(z)$:

$$\zeta(z) = \frac{1}{\Gamma(z)} \int_0^\infty \frac{x^{z-1}}{e^x - 1} dx, \tag{2.82}$$

where $\Gamma(z)$ is the Gamma function. Solving the equation above for the integral we achieve:

$$\zeta(z)\Gamma(z) = \int_0^\infty \frac{x^{z-1}}{e^x - 1} dx. \tag{2.83}$$

Hence, we can identify this integral in Eq. 5.12 for $z = 3/2$ so that:

$$\zeta(3/2)\Gamma(3/2) = \int_0^\infty \frac{x^{1/2}}{e^x - 1} d\varepsilon, \tag{2.84}$$

and N becomes:

$$N = C(k_B T_c)^{3/2} \zeta(3/2)\Gamma(3/2), \tag{2.85}$$

where $\zeta(3/2) = 2.612$ and $\Gamma(3/2) = \pi^{1/2}/2$, so finally:

$$N = C(k_B T_c)^{3/2} (\pi^{1/2}/2)(2.612). \tag{2.86}$$

Recalling that $C = \dfrac{2\pi}{h^3}(2m)^{3/2} v$, we have:

$$N = \frac{1}{h^3}(2m)^{2/3} v (k_B T_c)^{3/2} (\pi^{3/2})(2.612), \tag{2.87}$$

by solving for $k_B T_c$ we find the analytical expression for the critical temperature:

$$\boxed{k_B T_c = \left(\frac{N}{v}\right)^{2/3} \frac{h^2}{\pi (2.612)^{2/3} 2m}.} \tag{2.88}$$

It is also possible to determine an alternative expression for the ground state occupancy in terms of T_c. First, let us denote the total number N by adding the number of particles in the ground state $\langle n_1 \rangle$ and in the remaining excited states, considering they are both finite positive numbers:

$$N = \langle n_1 \rangle + \sum_{\alpha \geqslant 2} \langle n_\alpha \rangle . \tag{2.89}$$

Once again, rewriting the sum as an integral over a continuous energy spectrum:

$$N = \langle n_1 \rangle + \int_0^\infty \langle n_\alpha \rangle \, D(\varepsilon) d\varepsilon. \tag{2.90}$$

To proceed further we must discuss a useful approximation in this context. According to Ref. [5], ε_1 is of the order of 10^{-18} in a way that such a small number can be neglected when evaluating certain calculations so we can approximate this result to $\varepsilon_1 = 0$. With that in mind, note that for low temperatures when $\mu \to \varepsilon_1$ we can also approximate $\mu = 0$. This approximation is extremely useful in the thermodynamic analysis of such systems. That is because we are able to solve integrals of the type that appear in Eq. 2.80 for all values of T and not just for $T = T_c$. Hence, Eq. 2.90 becomes:

$$N = \langle n_1 \rangle + \int_0^\infty \frac{1}{e^{\varepsilon_\alpha / k_B T} - 1} D(\varepsilon) d\varepsilon. \tag{2.91}$$

Note that we can maintain the lower limit of integration as 0 because the integral evaluated at such a condition does not contribute to N. This means that we are not counting $\langle n_1 \rangle$ more than on time. The integral in the second term has already been solved for $T = T_c$ in the steps in which we derived an expression for the critical temperature.

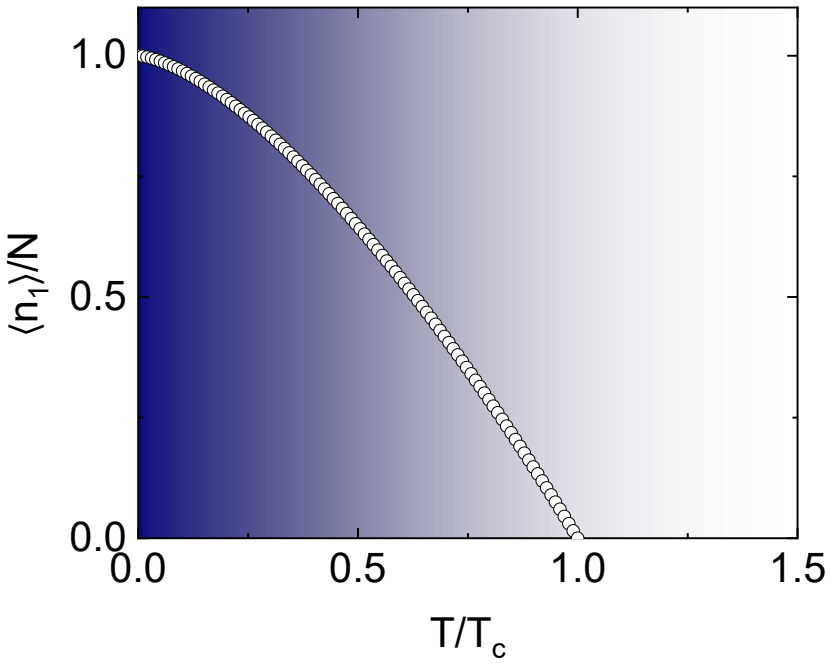


Figure 2 – Ratio between the expected occupancy of the ground state and the total number of particles $\frac{\langle n_1 \rangle}{N}$ as a function of the relative temperature $\frac{T}{T_c}$. It can be noted that for $T = T_c$, the condensation begins to take place. As the temperature goes to zero, $\langle n_1 \rangle / N$ goes to 1. The color gradient indicates that the condensation happens gradually as the temperature is reduced. Figure adapted from Ref. [5].

By solving this integral through the same reasoning but now for a given value of T in the low-temperature regime, we have:

$$\int_0^\infty \frac{1}{e^{\varepsilon_\alpha / k_B T} - 1} D(\varepsilon) d\varepsilon = \text{constant} \ \times T^{3/2}, \tag{2.92}$$

where the constant is given by all the constants multiplying $T_c^{3/2}$ in Eq. 2.87. Following our discussions, we saw that the condensation starts to happen at $T = T_c$ in a way that for such conditions, all the particles remain in the excited states, and as a consequence the integral in Eq. 2.92 must yield the total number of particles N. For that to happen tha constant multiplying $T^{3/2}$ must be expressible in the form $N/(T_c)^{3/2}$. Hence it is clear that such constant can be written as $N \left(\frac{T}{T_c} \right)^{3/2}$, so finally Eq. 2.91 becomes:

$$N = \langle n_1 \rangle + \left(\frac{T}{T_c} \right)^{3/2} N, \tag{2.93}$$

which we can solve for $\langle n_1 \rangle$ and ahive:

$$\langle n_1 \rangle = N \left[1 - \left(\frac{T}{T_c} \right)^{3/2} \right]. \tag{2.94}$$

Analyzing the limiting cases of the expression above we conclude that for $T = T_c$, the occupancy of the ground state is zero, and for $T \to 0$, $\langle n_1 \rangle = N$. Fig. 2 showcases the behavior being discussed. So if we start with a temperature $T > T_c$ and gradually reduce it to T_c, the particles will lose energy until a certain point at which they will begin to slowly occupy the ground state, up until the point at we reach $T = 0$ and all of the particles are in fact in the ground state. Suppose now that we start at $T = 0$ and gradually increase the temperature, the particles will gain energy and slowly occupy the excited states, and we reach $T = T_c$ from below, all the particles will have left the ground state. The color gradient in Fig. 2 indicates the gradual character of the condensation. Clearly Eq. 2.94 is only valid for $T < T_c$ following the limitations of the approximation $\mu = 0$.

2.6 ACCESSING THE THERMODYNAMICS OF THE IDEAL BEC

By computing an analytical expression for the total energy of the system we can access and analyze the thermodynamic properties of the ideal BEC. Recalling the previous section, we have that the total energy is [5]:

$$\langle E \rangle = \sum_{\alpha} \varepsilon_\alpha \langle n_\alpha \rangle . \tag{2.95}$$

By considering a temperature $T < T_c$, we can separate the energy contributions of the ground state E_1 and the remaining excited states $E_{\alpha \geqslant 2}$ to the total energy, so that:

$$\langle E \rangle = E_1 + E_{\alpha \geqslant 2}, \tag{2.96}$$

$$\langle E \rangle = \varepsilon_1 \langle n_1 \rangle + \int_0^\infty \frac{\varepsilon}{e^{(\varepsilon-\mu)/k_B T} - 1} D(\varepsilon) d\varepsilon, \tag{2.97}$$

$$\langle E \rangle = \varepsilon_1 N \left[1 - \left(\frac{T}{T_c} \right)^{3/2} \right] + \int_0^\infty \frac{\varepsilon}{e^{(\varepsilon/k_B T - \mu)} - 1} D(\varepsilon) d\varepsilon, \tag{2.98}$$

once again, we substituted the sum over all states by an integral with the density of states. Approximating $\mu = 0$, we have that:

$$E_{\alpha \geqslant 2} = \int_0^\infty \frac{\varepsilon}{e^{\varepsilon_\alpha / k_B T_c} - 1} D(\varepsilon) d\varepsilon. \tag{2.99}$$

The integral above can easily be solved in a similar way as the ones above. Replacing $x = \varepsilon / k_B T$ and recalling that $D(\varepsilon) = C\varepsilon^{1/2}$ and that such integral is a tabulated one, we have:

$$E_{\alpha \geqslant 2} = C(k_B T)^{5/2} \int_0^\infty \frac{x^{3/2}}{e^x - 1} dx, \tag{2.100}$$

$$E_{\alpha \geqslant 2} = C(k_B T)^{5/2} \zeta(5/2) \Gamma(5/2). \tag{2.101}$$

Looking back to Eq. 2.85 and solving it for C, we can write $C = \dfrac{N}{(k_B T_c)^{3/2} \zeta(3/2) \Gamma(3/2)}$. So we have:

$$E_{\alpha \geqslant 2} = (k_B T)^{5/2} \frac{N}{(k_B T_c)^{3/2}} \frac{\zeta(5/2)\Gamma(5/2)}{\zeta(3/2)\Gamma(3/2)}, \tag{2.102}$$

where $\dfrac{\zeta(5/2)\Gamma(5/2)}{\zeta(3/2)\Gamma(3/2)} = 0.770$ [24]. Thus we achieved:

$$E_{\alpha\geqslant 2} = 0.770N\frac{(k_BT)^{5/2}}{(k_BT_c)^{3/2}} = 0.770\frac{(T)^{5/2}}{(T_c)^{3/2}}Nk_B. \tag{2.103}$$

Hence, the complete expression that gives the total energy of the system in terms of the temperature is:

$$\boxed{\langle E\rangle = \varepsilon_1 N\left[1-\left(\frac{T}{T_c}\right)^{3/2}\right] + 0.770\frac{(T)^{5/2}}{(T_c)^{3/2}}Nk_B.} \tag{2.104}$$

With such relation at our disposal, we can now compute many observable properties of the system like heat capacity at constant volume, which can be accessed through the expression:

$$\left(\frac{\partial\langle E\rangle}{\partial T}\right)_v = 1.925Nk_B\left(\frac{T}{T_c}\right)^{3/2} - \frac{3}{2T_c}\varepsilon_1 N\left(\frac{T}{T_c}\right)^{1/2}. \tag{2.105}$$

Recalling that ε_1 is a small number, we achieve the result that for $T < T_c$, c_v grows as $T^{3/2}$.

3 ANALYSING THE EFFECTS OF INTERACTION IN THE BOSE-EINSTEIN CONDENSATE

In the last chapter, through a simple analysis of the Bose-Einstein distribution, we could achieve interesting results concerning the thermodynamical behavior of the ideal Bose gas. Even though the analysis of the ideal case provides satisfactory results, in the real world particles “feel" the presence of each other. With that in mind, in this section, we aim to revisit the framework of the interacting Bose gas.

3.1 ACCESSING THE THERMODYNAMICS OF THE NON-IDEAL BEC

Our main goal in this section, following the discussions in Pathria's and Landau's books, will be to compute an expression for the system's free energy F, from which we can derive thermodynamic quantities of interest. We start from the Hamiltonian $\hat{H}$ that describes a number of bosons which interact through a scattering potential $\hat{U}(r)$:

$$\hat{H} = \sum_{\mathbf{p}} \frac{p^2}{2m} \hat{a}^\dagger_{\mathbf{p}} \hat{a}_{\mathbf{p}} + \frac{1}{2} \sum_{\mathbf{p}} \langle \mathbf{p_1'}, \mathbf{p_2'} | \, \hat{U}(r) \, | \mathbf{p_1}, \mathbf{p_2} \rangle \, \hat{a}^\dagger_{\mathbf{p_1'}} \hat{a}^\dagger_{\mathbf{p_2'}} \hat{a}_{\mathbf{p}_1} \hat{a}_{\mathbf{p}_2}, \tag{3.1}$$

where $\hat{a}^\dagger_{\mathbf{p}}$ and $\hat{a}_{\mathbf{p}}$ are the creation and anhilation operators of particles with momentum $\mathbf{p}$. The first term in the Hamiltonian is the kinetic term, incorporating the energy transferred in a scattering process with a transfer of momentum $\mathbf{p}$. The second term refers to the potential energy, which in this case is a scattering potential. We can interpret the product of the four operators as the scattering of two particles, which start with momentum $\mathbf{p_1}$ and $\mathbf{p_2}$ and acquire a momentum $\mathbf{p'_1}$ and $\mathbf{p'_2}$ after the scattering process. The matrix element $\langle \mathbf{p_1'}, \mathbf{p_2'} | \, \hat{U}(r) \, | \mathbf{p_1}, \mathbf{p_2} \rangle$ is given by:

$$\langle \mathbf{p_1'}, \mathbf{p_2'} | \, \hat{U}(r) \, | \mathbf{p_1}, \mathbf{p_2} \rangle = \frac{1}{v} \int \hat{U}(r) e^{i\mathbf{p}\cdot\mathbf{r}} d^3 r. \tag{3.2}$$

This Hamiltonian, in its most general form, cannot be solve analytically. Fortunately, the complexity of the problem is reduced under the light of the celebrated Born approximation, which considers the scattering potential $\hat{U}(r)$ as a perturbation of the system [21]. This approximation is made by assuming that the range of the scattering potential is way smaller than the actual distance between particles [15]. These considerations exist in a system in which the particles hardly ever notice each other, hence we may call this system a diluted Bose gas. Recalling perturbation theory, the matrix elements of a perturbation $\hat{V}$ in a Hamiltonian can be written in terms of its m order corrections. The second order correction is given by:

$$V_{ij} = V_{00} + \sum_{n \neq 0} \frac{V_{0n} V_{n0}}{E_0 - E_n} + ..., \tag{3.3}$$

where the first term represents the first order correction [21]. The difference between the unperturbed and perturbed wave functions is essentially the value of its momentum since the scattering potential is considered as a perturbation [14]. Before the scattering, both particles carrie momenta $\mathbf{p_1}$ and $\mathbf{p_2}$ (unperturbed). After the scattering occurs, the momenta become $\mathbf{p_1'}$ and $\mathbf{p_2'}$ (perturbed). Due to the conservation of momentum, we express the amount of it transferred in this process by $\mathbf{p} = (\mathbf{p_2} - \mathbf{p_2'}) = -(\mathbf{p_1} - \mathbf{p_1'})$ [14]. Hence, the first order correction, which refers to the matrix elements with respect to the unperturbed wave functions, becomes:

$$\langle \mathbf{p_1}, \mathbf{p_2} | \, \hat{U}(r) \, | \mathbf{p_1}, \mathbf{p_2} \rangle = \frac{1}{v} \int \hat{U}(r) e^{i(0)\cdot \mathbf{r}} d^3 r = \frac{U_0}{v}. \tag{3.4}$$

where U_0 is the force associated to such scattering process [26]. With this analysis, we have demonstrated that the first order correction to the perturbation $\hat{U}(r)$ takes into account only scatterings which involve $\mathbf{p} = \mathbf{0}$. This is an important result because it indicates to us that this approximation is only valid in conditions where the collisions associated with the scattering process are very slow. This constraint shows us that this approximation is only valid in low-temperature regimes where the thermal energy is so low that the collisions between particles transfer no momentum whatsoever [14]. In order to continue, we recall the relation between the scattering length a and the potential, which in the low-temperature regime, becomes:

$$a = \frac{m}{4\pi\hbar^2} = \int \hat{U}(r) e^{i(0)\cdot \mathbf{r}} d^3 r = \frac{m}{4\pi\hbar^2} U_0, \tag{3.5}$$

where $\hbar = \dfrac{h}{2\pi}$ [14]. If the scattering length is negative, the scattering potential is said to be attractive. If a is positive, then the potential is repulsive [15]. By substituting $\hat{U}(r)$ for its first order correction in the Hamiltonian, i.e., U_0/v, and then writing U_0 in terms of a we come to:

$$\hat{H} = \sum_{\mathbf{p}} \frac{p^2}{2m} \hat{a}^\dagger_{\mathbf{p}} \hat{a}_{\mathbf{p}} + \frac{2\pi a \hbar^2}{mv} \sum_{\mathbf{p_1}, \mathbf{p_2}} \hat{a}^\dagger_{\mathbf{p}_1'} \hat{a}^\dagger_{\mathbf{p}_2'} \hat{a}_{\mathbf{p}_1} \hat{a}_{\mathbf{p}_2}. \tag{3.6}$$

Due to the fact that we are analyzing this Hamiltonian in the first approximation, we need to evaluate the sums with caution because now the four operators represent scatterings in which no momentum is transferred so the values of $\mathbf{p}$ are no longer arbitrary. This constraint can be imposed by writing the Hamiltonian as:

$$\hat{H} = \sum_{\mathbf{p}} \frac{p^2}{2m} \hat{a}^\dagger_{\mathbf{p}} \hat{a}_{\mathbf{p}} + \frac{2\pi a \hbar^2}{mv} \left[\sum_{\mathbf{p}} \hat{a}^\dagger_{\mathbf{p}} \hat{a}^\dagger_{\mathbf{p}} \hat{a}_{\mathbf{p}} \hat{a}_{\mathbf{p}} + \sum_{\mathbf{p_1}, \mathbf{p_2}} \left(\hat{a}^\dagger_{\mathbf{p}_1} \hat{a}^\dagger_{\mathbf{p}_2} \hat{a}_{\mathbf{p}_2} \hat{a}_{\mathbf{p}_1} + \hat{a}^\dagger_{\mathbf{p}_2} \hat{a}^\dagger_{\mathbf{p}_1} \hat{a}_{\mathbf{p}_2} \hat{a}_{\mathbf{p}_1} \right) \right]. \tag{3.7}$$

Note that the three products involving the $\hat{a}$ and $\hat{a}^\dagger$ operators all represent scatterings in which no momentum is transferred. In the first one, two particles with the same momenta are annihilated and created with the same amount of such momenta. The second term refers to scatterings in which two particles with two different initial momenta are scattered and unaffected by such process and maintain their initial value of momentum. The third

one represents a scattering in which the particles acquire the momentum of each other. In this scenario, we have a particle with momentum $\mathbf{p_1}$ being annihilated and created again, with the same being true for the particle with $\mathbf{p_2}$. Hence, this process corresponds to a scattering with no momentum transfer. All these scattering processes are represented schemetically in Fig. 3. We can work on these products of four operators if we recall the commutation relations obeyed by such operators [14], which read:

$$[a_\alpha, a_\beta^\dagger] = \delta_{\alpha\beta}; \quad [a_\alpha, a_\beta] = [a_\alpha^\dagger, a_\beta^\dagger] = 0, \tag{3.8}$$

where $\delta_{\alpha\beta}$ is a Kronecker delta and α and β are arbitrary indicies [24]. Additionally, we also recall that the product of the operators $a_\alpha^\dagger$ and a_α yields the particle number operator of a state α, represented by $\hat{n}_\alpha = a_\alpha^\dagger a_\alpha$ [14]. Whereas the linear combination of these products yields the total number of particles operator $\hat{N} = \sum_\alpha a_\alpha^\dagger a_\alpha$. The eigenvalues of such operators are naturally the number of particles in a state α, n_α, and the total number of particles N [27]. The commutators of $\hat{n}_\alpha$ with $a_\alpha^\dagger$ and a_α are:

$$[a_\alpha^\dagger, \hat{n}_\alpha] = a_\alpha; \quad [a_\alpha, \hat{n}_\alpha] = -a_\alpha^\dagger. \tag{3.9}$$

With these relations in mind, we can rewrite the products of four operators. Starting with the first sum in Eq. 3.7, we have:

$$\sum_{\mathbf{p}} a_{\mathbf{p}}^\dagger a_{\mathbf{p}} a_{\mathbf{p}}^\dagger a_{\mathbf{p}} = \sum_{\mathbf{p}} a_{\mathbf{p}}^\dagger (a_{\mathbf{p}}^\dagger a_{\mathbf{p}} - 1) a_{\mathbf{p}}, \tag{3.10}$$

where $(a_{\mathbf{p}}^\dagger a_{\mathbf{p}} - 1)$ comes from the first relation in Eq. 3.8. By applying the distributive property, we achieve:

$$\sum_{\mathbf{p}} a_{\mathbf{p}}^\dagger (a_{\mathbf{p}}^\dagger a_{\mathbf{p}} - 1) a_{\mathbf{p}} = \sum_{\mathbf{p}} a_{\mathbf{p}}^\dagger a_{\mathbf{p}} a_{\mathbf{p}}^\dagger a_{\mathbf{p}} - a_{\mathbf{p}}^\dagger a_{\mathbf{p}} = \sum_{\mathbf{p}} \hat{n}_{\mathbf{p}}^2 - \hat{n}_{\mathbf{p}} = \sum \hat{n}_{\mathbf{p}}^2 - \hat{N}. \tag{3.11}$$

Following a similar procedure, the second sum in Eq. 3.7 can be rewritten knowing that $\hat{a}_{\mathbf{p}_2} \hat{a}_{\mathbf{p}_1} = \hat{a}_{\mathbf{p}_1} \hat{a}_{\mathbf{p}_2}$ and also that $\hat{a}_{\mathbf{p}_2}^\dagger \hat{a}_{\mathbf{p}_1} = \hat{a}_{\mathbf{p}_1} \hat{a}_{\mathbf{p}_2}^\dagger$. Hence, we have:

$$\sum_{\mathbf{p_1},\mathbf{p_2}} \hat{a}_{\mathbf{p}_1}^\dagger \hat{a}_{\mathbf{p}_2}^\dagger \hat{a}_{\mathbf{p}_2} \hat{a}_{\mathbf{p}_1} = \sum_{\mathbf{p_1},\mathbf{p_2}} a_{\mathbf{p}_1}^\dagger \hat{a}_{\mathbf{p}_2}^\dagger \hat{a}_{\mathbf{p}_1} \hat{a}_{\mathbf{p}_2} = \sum_{\mathbf{p_1},\mathbf{p_2}} a_{\mathbf{p}_1}^\dagger \hat{a}_{\mathbf{p}_1} \hat{a}_{\mathbf{p}_2}^\dagger \hat{a}_{\mathbf{p}_2}, \tag{3.12}$$

which we can further develop by recalling $\hat{n}_\alpha = a_\alpha^\dagger a_\alpha$, so it follows that:

$$\sum_{\mathbf{p_1},\mathbf{p_2}} a_{\mathbf{p}_1}^\dagger \hat{a}_{\mathbf{p}_2}^\dagger \hat{a}_{\mathbf{p}_1} \hat{a}_{\mathbf{p}_2} = \sum_{\mathbf{p_1},\mathbf{p_2}} \hat{n}_{\mathbf{p_1}} \hat{n}_{\mathbf{p_2}} = \sum_{\mathbf{p_1},\mathbf{p_2}} \hat{n}_{\mathbf{p_1}} (\hat{N} - \hat{n}_{\mathbf{p_1}}) = \hat{N}^2 - \sum_{\mathbf{p}} \hat{n}_{\mathbf{p}}^2. \tag{3.13}$$

The third and last sum in Eq. 3.7 is essentially the same as the second one. To go from one to the other we only need to commute $a_{\mathbf{p}_1}^\dagger \hat{a}_{\mathbf{p}_2}^\dagger$ with $a_{\mathbf{p}_2}^\dagger \hat{a}_{\mathbf{p}_1}^\dagger$. Hence, the result in Eq. 3.13 is also valid for such a term. So we have:

$$\sum_{\mathbf{p_1},\mathbf{p_2}} \hat{a}_{\mathbf{p}_2}^\dagger \hat{a}_{\mathbf{p}_1}^\dagger \hat{a}_{\mathbf{p}_2} \hat{a}_{\mathbf{p}_1} = \sum_{\mathbf{p_1},\mathbf{p_2}} = a_{\mathbf{p}_1}^\dagger \hat{a}_{\mathbf{p}_2}^\dagger \hat{a}_{\mathbf{p}_1} \hat{a}_{\mathbf{p}_2} = \hat{N}^2 - \sum_{\mathbf{p}} \hat{n}_{\mathbf{p}}^2. \tag{3.14}$$

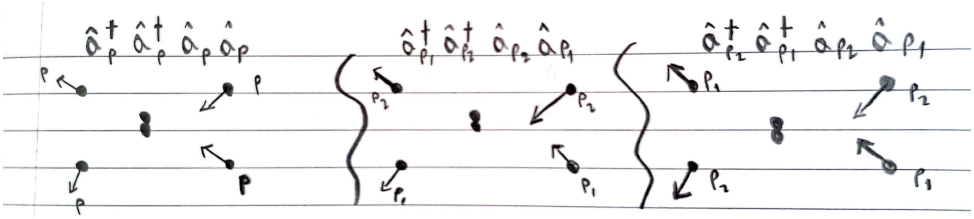


Figure 3 – Schematic representation of the scattering processes which involve a null momentum transfer. Adapted from Ref. [14].

By substituting Eqs. 3.11, 3.13, 3.14 in the hamiltonian, we achieve:

$$\hat{H} = \sum_{\mathbf{p}} \frac{p^2}{2m}\hat{n}_{\mathbf{p}} + \frac{2\pi a\hbar^2}{mv}\left[\cancel{\sum_{\mathbf{p}} \hat{n}_{\mathbf{p}}^2} - \hat{N} + \hat{N}^2 - \cancel{\sum_{\mathbf{p}} \hat{n}_{\mathbf{p}}^2} + \hat{N}^2 - \sum_{\mathbf{p}} \hat{n}_{\mathbf{p}}^2\right]. \tag{3.15}$$

$$\hat{H} = \sum_{\mathbf{p}} \frac{p^2}{2m}\hat{n}_{\mathbf{p}} + \frac{2\pi a\hbar^2}{mv}\left[2\hat{N}^2 - \hat{N} - \sum_{\mathbf{p}} \hat{n}_{\mathbf{p}}^2\right]. \tag{3.16}$$

Now that we have a Hamiltonian written in terms of the operators $\hat{N}$ and $\hat{n}_{\mathbf{p}}$ and we know exactly what the eigenvalues of such operators, the eigenenergies are:

$$E_{\{n_{\mathbf{p}}\}} = \sum_{\mathbf{p}} \frac{p^2}{2m} n_{\mathbf{p}} + \frac{2\pi a\hbar^2}{mv}(2N^2 - N - \sum_{\mathbf{p}} n_{\mathbf{p}}^2), \tag{3.17}$$

which can be approximated to:

$$E_{\{n_{\mathbf{p}}\}} = \sum_{\mathbf{p}} \frac{p^2}{2m} n_{\mathbf{p}} + \frac{2\pi a\hbar^2}{mv}(2N^2 - n_0^2), \tag{3.18}$$

following that $N - \sum_{\mathbf{p}} n_{\mathbf{p}}^2 \simeq n_0^2$, where n_0 is the number of particles in the ground state [14]. From the expression above, we can probe an expression for the system's ground state. For $T = 0$, we have that the number of particles in excited states with momentum $n_{\mathbf{p}}$ is zero cf. the discussions in the last chapter. Naturally under this condition, $n_0 = N$ and so we have:

$$E_0 = \frac{2\pi a\hbar^2 N^2}{mv}. \tag{3.19}$$

With the eigenenergies in hands, we can compute the system's partition function Z_N through:

$$Z_N = \sum_{\{n_{\mathbf{p}}\}} \exp(-\beta E_{\{n_{\mathbf{p}}\}}) = \ln \sum_{\{n_{\mathbf{p}}\}} \exp\left\{-\beta\left[\sum_{\mathbf{p}} \frac{p^2}{2m} n_{\mathbf{p}} + \frac{2\pi a\hbar^2}{mv}(2N^2 - n_0^2)\right]\right\}. \tag{3.20}$$

To finally access the free energy F, we must compute the logarithm of the partition function, so that:

$$\ln Z_N = \ln \sum_{\{n_{\mathbf{p}}\}} \exp(-\beta E_{\{n_{\mathbf{p}}\}}) = \sum_{\{n_{\mathbf{p}}\}} \exp\left\{-\beta\left[\sum_{\mathbf{p}} \frac{p^2}{2m} n_{\mathbf{p}} + \frac{2\pi a\hbar^2}{mv}(2N^2 - n_0^2)\right]\right\}, \tag{3.21}$$

$$\ln Z_N = \ln \sum_{\{n_{\mathbf{p}}\}} \left\{ \exp\left[-\beta \sum_{\mathbf{p}\neq\mathbf{0}} \frac{p^2}{2m} n_{\mathbf{p}} \right] \exp\left[\frac{-2\beta\pi a\hbar N^2}{mv} \left(2 - \frac{n_0^2}{N^2} \right) \right] \right\}. \tag{3.22}$$

Note that the term $\exp\left[\frac{-2\beta\pi a\hbar N^2}{mv} \left(2 - \frac{n_0^2}{N^2} \right) \right]$ does not take part in any of the sums, so we may write:

$$\ln Z_N = \ln \left\{ \exp\left[\frac{-2\beta\pi a\hbar N^2}{mv} \left(2 - \frac{n_0^2}{N^2} \right) \right] \sum_{\{n_{\mathbf{p}}\}} \exp\left[-\beta \sum_{\mathbf{p}} n_{\mathbf{p}} \frac{p^2}{2m} \right] \right\}, \tag{3.23}$$

based on the fact that $\log(ab) = \log(a) + \log(b)$, the logarithm of the partition function becomes:

$$\ln Z_N = \ln \exp\left[\frac{-2\beta\pi a\hbar N^2}{mv} \left(2 - \frac{n_0^2}{N^2} \right) \right] + \ln \sum_{\{n_{\mathbf{p}}\}} \exp\left[-\beta \sum_{\mathbf{p}} n_{\mathbf{p}} \frac{p^2}{2m} \right]. \tag{3.24}$$

The second term is simply the logarithm of the partition for the ideal quantum gas $\ln Z_{N_{(ideal)}}$ [14]. That is because it corresponds to a system where the only energy scale present is the one associated with the kinetic energy. so we have:

$$\ln Z_N = \ln Z_{N_{(ideal)}} - \frac{2\beta\pi a\hbar N^2}{mv} \left(2 - \frac{n_0^2}{N^2} \right). \tag{3.25}$$

Plugging Eq. 3.25 in $F = -k_B T \ln Z_N$, we achieve the system's free energy:

$$F = -k_B T \ln Z_{N_{(ideal)}} + k_B T \frac{2\beta\pi a\hbar N^2}{mv} \left(2 - \frac{n_0^2}{N^2} \right). \tag{3.26}$$

From this expression, all the thermodynamic quantities of interest can be obtained. Additionally, we can extract some useful information about this system if we recall the relation between n_0/N and the thermal de Broglie wavelength λ [14], which is given by:

$$\frac{n_0}{N} = 1 - \frac{\lambda_c^3}{\lambda^3}., \tag{3.27}$$

where λ_c is a fixed critical value of λ associated to T_c. Thus the expression of F in terms of λ is:

$$F = -k_B T \ln Z_{N_{(ideal)}} + k_B T \frac{2\beta\pi a\hbar N^2}{mv} \left[2 - \left(1 - \frac{\lambda_c^3}{\lambda^3} \right)^2 \right], \tag{3.28}$$

$$\boxed{F = -k_B T \ln Z_{N_{(ideal)}} + k_B T \frac{2\beta\pi a\hbar N^2}{mv} \left(1 - 2\frac{\lambda_c^3}{\lambda^3} + \frac{\lambda_c^6}{\lambda^6} \right).} \tag{3.29}$$

Analyzing this expression we can see that the free energy of the system is simply its ideal component added to a correction associated with the interactions. Furthermore, the term related to the interactions depends on the negative powers of λ. Recalling that $\lambda \propto 1/T$, we can see that for low temperatures these terms are really small, which means that the interactions hardly affect the thermodynamics of the system [14]. This statement is in accordance with the fact that the scattering potential was considered to be a mere

perturbation in the Hamiltonian. Interestingly, there is a term with no dependence on T, this term refers to the ground state energy of the system. Hence we have achieved our goal of computing the free energy of an interacting Bose gas, however, many approximations had to be made. For a more accurate description of this system, higher-order corrections of the perturbation would be necessary, which be done at the cost of increasing the problem's complexity.

3.2 THE BRILLOUIN PARAMAGNET AND THE BOSE-EINSTEIN CONDENSATION

The Brillouin paramagnet is a model used to describe the paramagnetic properties of non-interacting localized particles [5]. For a system with one particle with angular momentum $J = 1/2$, its partition function is given by:

$$Z_N = \left[e^{\frac{\mu_B B}{k_B T}} + e^{-\frac{\mu_B B}{k_B T}} \right], \tag{3.30}$$

where μ_B is Bohr's magneton and B the applied magnetic field. Through trigonometric relations, we can write the partition function as:

$$Z_N = \left[2\cosh\left(\frac{\mu_B B}{k_B T}\right) \right]. \tag{3.31}$$

Recalling that F is connected to Z_N by $F = -k_B T \ln(Z_N)$, it becomes possible to compute the system's entropy using the relation $S = -\left(\frac{\partial F}{\partial T}\right)_{N,B}$. Hence, we have:

$$S(T, B) = k_B \left\{ \ln\left[2\cosh\left(\frac{\mu_B B}{k_B T}\right) \right] - \frac{\mu_B B}{k_B T} \tanh\left(\frac{\mu_B B}{k_B T}\right) \right\}. \tag{3.32}$$

The following discussion is based on Ref. [11]. By taking the limit $B \to 0$, the entropy takes the value

$$S(T, 0) = k_B \ln(2). \tag{3.33}$$

For $B = 0$, the entropy loses its temperature dependence and furthermore, it becomes finite as the $T \to 0$. Such a scenario violates the third law of Thermodynamics [17]. It was proposed in Ref. [11] that to contour this situation it becomes necessary to take the interactions between spins into account. As $T \to 0$, the energy scale associated with the dipolar interaction between spins becomes more expressive. Such interaction is responsible for the emergence of a local magnetic field B_{loc} which allings the spins in its direction. The alignment of the spins clearly favors the ordering of the system. Thus, it becomes possible to conclude that the ground state of a Brillouin paramagnet is in fact a ferromagnet.

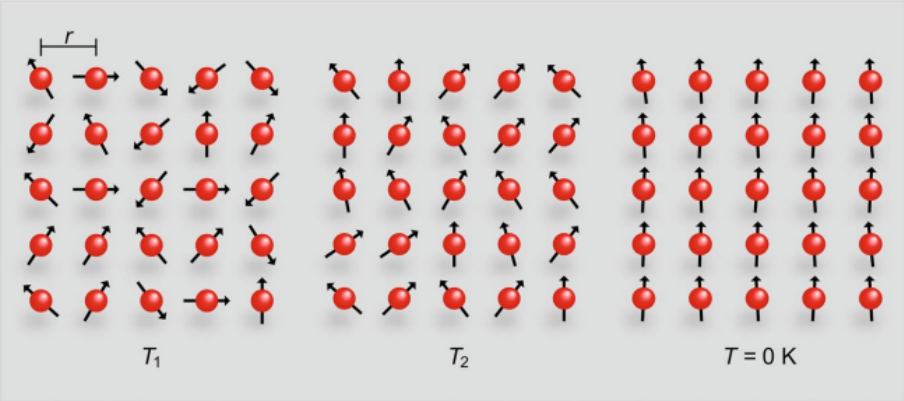


Figure 4 – Schematic representation of the appearance of the ferromagnetic phase in the Brillouin paramagnet, due to the presence of the local field B_{loc} which is originated by the magnetic dipolar interactions. As the temperature is reduced, cf. $T_1 > T_2$, the magnetic energy becomes more expressive than the thermal scale and thus the particles align themselves according to B_{loc} for $T = 0$. Figure taken from Ref. [11].

Mathematically, we can replace B in the entropy expression by $B_r = \sqrt{B_{loc} + B}$, which incorporates both the external field applied to the system and the local field produced by the interactions. Hence, when $B = 0$, the entropy is temperature-dependent and the Third Law of Thermodynamics is not violated. The establishment of a ferromagnetic regime was identified as an analogous phenomenon of a BEC. Hence the goal of this section is to explore the connections and similarities between both phenomena in order to clearly state the role played by interactions in the BEC. As we have discussed in the former section, the particles in Bose-Einstein condensate interact through the process of scattering [15]. The scattering length a was obtained through the Born approximation which implicates in diluted systems so the collisions between particles are quite rare [21]. Hence, the effects of such interaction are not expressive. However, in a system with a higher density, the rate of collisions is dramatically enhanced [28]. In such scenarios the effect of interactions becomes essential to the manifestation of the BEC [27]. It was mentioned in the last section that what dictated whether the scattering potential was attractive or repulsive was the sign of the scattering length a [15]. Interestingly, the attractiveness or repulsiveness of the scattering potential dictates the manifestation of the BEC [27]. By lowering T, the energy scale associated with the kinetic energy becomes less expressive. In such conditions, the energy scale associated with the scattering potential starts to dominate the system, and thus a competition between the attractive and repulsive potential sets in. In the attraction regime, as T is reduced, the particles of the system condense in the system's ground state and also come close to each other, as a consequence of the attraction potential becoming more expressive. Hence, this grouping of particles in a single point gives rise to an energetical instability which causes the condensate wave function to split [27].

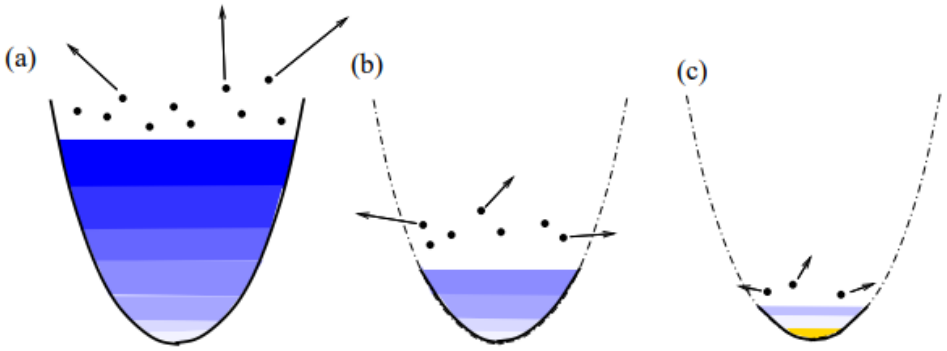


Figure 5 – Schematic representation of evaporative cooling of harmonic trapped particles. In (a) particles are imprisoned by the potential. The color gradient indicates higher energy levels of such potential. In (b) the energy scale associated with the potential is being reduced which is represented by the appearance of dashed lines thus allowing the faster particles to escape, indicated by the arrows. The scaping particles carry away the thermal energy and thus the system is cooled. (c) A small number of very slow particles are left in the system. Figure taken from Ref. [29].

In Dirac's notation, the ket associated with the ground state $|\Psi\rangle$ can be constructed with N applications of the operator $a_\theta^\dagger$ in the vacuum state $|0\rangle$. When $a_\theta^\dagger$ acts on $|0\rangle$ a particle in a state $|\theta\rangle$ is created. The state $|\theta\rangle$ is the first vector of a basis $|\theta_k\rangle$. Since only acts on θ we have an assembling of particles in the first basis vector of $|\theta_k\rangle$. Hence, the wave function of a Bose-Einstein condensate in Dirac's notation is given by [27]:

$$|\Psi\rangle = \frac{1}{\sqrt{N!}}[a_\theta^\dagger]\,|0\rangle\,, \tag{3.34}$$

where $1/\sqrt{N!}$ is a normalization constant. The mentioned instability causes $|\Psi\rangle$ to split all of its particles into other states of the basis $|\theta_k\rangle$ in order to restore equilibrium. Denoting two different vectors of such basis by $|\theta_a\rangle$ and $|\theta_b\rangle$, we have that the wave function of a split condensate is:

$$|\Psi\rangle = \frac{1}{\sqrt{N_a!N_b!}}[a_{\theta_a}^\dagger][a_{\theta_b}^\dagger]\,|0\rangle\,, \tag{3.35}$$

where $a_{\theta_a}^\dagger$ and $a_{\theta_b}^\dagger$ are the creation operators in the states $|\theta_a\rangle$ and $|\theta_b\rangle$. Under these conditions, the attractive potential is essential to the fragmentation of the condensate and thus essential to its establishment as a stable phase of the system. If $a > 0$, then the scattering potential causes the particles to move away from each other. This causes the particles to remain apart from each other and allows them to occupy the ground state with no instability. In this scenario $|\Psi\rangle$ remains intact and we have a stable condensate. Hence, we can see that the interaction between particles is essential to the stability and occurrence of the BEC [27]. With this discussion in mind, we can make a comparison between the BEC and the appearance of the ferromagnetic phase in the Brillouin paramagnet. In both cases, as T is reduced, the energy scale associated with the interactions becomes more expressive and thus favors the ordering of the system. On the frame of the BEC, the

establishment of this order manifests itself in the condensation. For the paramagnet case, the appearance of the ferromagnetic phase is the manifestation of the ordering of the system [11]. Interestingly, for the condensation of dipolar molecules, the dipolar interaction plays an analogous role as the scattering potential in determining the stability of the condensate [30]. In this sense, the dipolar molecular interaction acts on the BEC in the same manner as the dipolar magnetic interaction acts on the Brillouin paramagnet. The effects of interaction between particles also play a key role in the experimental realization of the BEC. For such experiments the process of evaporative cooling is essential for achieving the temperatures required for the condensation [9]. In this context, this cooling method is directly linked with harmonic trapped particles and consists essentially in lowering the energy scale associated with the trapping potential thus allowing the particles with a higher energy to escape. If we define a trapping energy of $\eta k_B T$, where η is the so-called truncation parameter, the particles which carry kinetic energy $\dfrac{p^2}{2m} \geqslant \eta k_B T$, will escape the trap [28]. Such escaping particles carry away thermal energy and thus the system is cooled. Hence, the rate at which the system is cooled is proportional to the number of elastic scattering processes that transfer an amount of energy $E \geqslant \eta k_B T$ [28]. For a constant η, the relation between the cooling rate $1/\tau_{ev}$ and the rate of such elastic collisions $1/\tau_{el}$ is linear and given by:

$$\lambda^* = \frac{\tau_{ev}}{\tau_{el}}, \tag{3.36}$$

where λ^* is a parameter that depends only on η and τ_{ev} and $1/\tau_{ev}$ are the time constants associated with the evaporation and scattering process [28]. We can write the latter as $1/\tau_{el} = nV\sigma$ where n is the particle density, V the speed of such particles, and σ the scattering cross-section. Thus, we have:

$$n\mathrm{v}\sigma = \frac{1}{1/\tau_{ev}}\lambda. \tag{3.37}$$

Note that if we increase the density, the cooling rate is enhanced due to an increase in the number of collisions, as expected. As a result of this enhancement in the cooling rate, T is reduced and thus the attractive/repulsive potentials become more expressive, and thus the processes discussed earlier in this section start to take place.

4 EXPERIMENTAL ASPECTS

In this chapter, we shall revisit major points concerning the experimental realization of a BEC, which include important physical concepts associated with the experiments and historical aspects. Furthermore, the experiments performed at the *Solid State Physics lab* will be discussed, due to their great importance in supplementing theoretical results.

4.1 INTIAL DISCUSSIONS AND PREDICTIONS

Before discussing the experimental character of BEC, we shall elucidate some major historical points that led to its first experimental realization. In the early 20th century, the physicist S. Bose managed to derive Planck's distribution law which describes the energy density irradiated by a black body in thermal equilibrium based on the framework of Statistical Mechanics [7]. At the time, the corpuscular character of electromagnetic radiation was already well established, so the work of Bose indicated that the formalism of Statistical Mechanics could be used to describe quantum phenomena. Bose sent a copy of his works to A. Einstein in 1924, who immediately recognized the importance of Bose's work and started to work on his own in what would be known in the future as Quantum Statistical Mechanics. Einstein realized that a system consisting of bosons, indistinguishable particles that hold an integer value of spin, would undergo a phase transition at extremely low temperatures as a result of the total suppression of thermal energy in the system [6]. Since N bosons are allowed to ocupate the same quantum state when $T \to 0$ all particles condense in the lowest energy state. All predictions made by Einstein in the 20s remained restricted to the theory alone because, at the time, no real system was known to present the physical characteristics of the condensate. It was only in 1938, that Fritz London conjectured that the superfluid transition of ^{4}He, was in fact an effect of BEC [5, 31]. The phase transition just mentioned is famously known as *lambda transition*, because the specific heat versus temperature graph (Fig. 6), has a similar form as the Greek letter lambda λ. London's suggestion was based on comparing the graphs of the lambda transition and the graph of the heat capacity as a function of the temperature of the ideal Bose gas, which have similar shapes. An interesting idea that came as a way of proving or disproving London's suggestion was to analyze the cooling of ^{3}He and check if a lambda transition would be observed. That is a good idea because these isotopes of Helium differ only by their net spin value, while ^{4}He has a net spin equal to zero, ^{3}He has a net spin of $(1/2)\hbar$. In other words, ^{4}He presents a bosonic character while ^{3}He a fermionic one. Hence, if ^{3}He does not go through a lambda transition, we can conclude that this is due to the fermionic character of ^{3}He. As it is now well known, ^{3}He does not present a

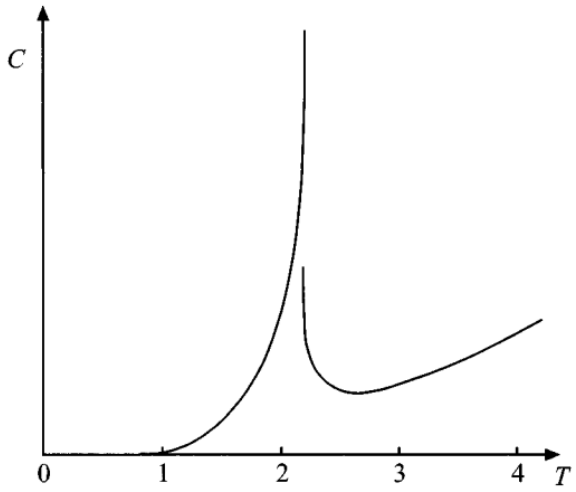


Figure 6 – Heat capacity of liquid ^{4}He as a function of temperature. At a temperature $T_\lambda = 2.17$ K, the system goes through a superfluid transition [32]. Figure taken from Ref. [5]

lambda transition at any temperature [32]. Thus we conclude that such phenomena are intrinsically connected to the bosonic character of ^{4}He.

4.2 INITIAL STEPS TOWARDS BEC EXPERIMENTS

The conclusion that 4He could manifest the BEC influenced the scientific community to search for other systems that would be appropriate to manifest a BEC and to develop a new experimental setup to do so. Obviously, the physical conditions for such experiments are very precise so the task would be no easy one. The breakthrough of laser physics was of extreme importance in this context, since the high intensity and dexterity of laser beams permitted the formulation of experiments with unprecedented precision. In 1968, V. S. Letokhov proposed trapping atoms with high-intensity electromagnetic fields [33], and in 1975 T. W. Hänsch and A. L. Schawlow suggested that laser beams could be used to cool down a system [34], these consist the two main ideas behind the first experimental realization of a BEC. The pioneer experiments that involved trapped atoms consisted of a three-dimensional laser setup known as optical molasses [35]. However, such traps were not efficient enough for a large number of atoms. A more sophisticated method was required to cool down many atoms and it was proposed in 1987 by y D. E. Pritchard's group in collaboration with S. Chu's group [36]. This new setup consisted of an optical trap combined with a magnetic field known as MOT (magneto-optical-trap) enabling the trapping of a larger number of atoms. As for the laser cooling, consisted of making the atoms move in the opposite direction of the beam in a way that they would collide with photons, absorb them, and thus lose speed. As we have already discussed, the process known as evaporative cooling proved itself efficient in this context. Another major concern at the time was the real system that could be used as a sample to manifest the condensation. One of the first candidates was the spin-polarized Hydrogen [37]. Since

this isotope of hydrogen contains nothing but one proton and one electron, their spins cancel each other in a way that the net spin of the atom is zero. An alternative to the spin-polarized hydrogen was the alkali metals, elements of the first column of the periodic table that have atoms with bosonic character due to their single valence electron, which is discussed in the next section.

4.3 CONDENSATION OF ALKALI DILUTED GASES

In 1995 at the University of Colorado, the JILA (Joint Institute for Laboratory Astrophysics) research group led by Carl Wieman, with the support of post-doc. Eric Cornell, produced the first BEC in history, using a dilute gas of rubidium atoms [38]. Upon cooling and trapping the Rb sample with the methods mentioned in the former subsection, temperatures on the scale of 170 nK could be achieved. The experiments in which a BEC was achieved consisted essentially of a combination of the two cooling techniques we discussed so far. The challenge was to understand how to combine these two techniques. That is because laser cooling is more efficient at low densities [9]. Higher densities would cause the laser beams to be absorbed by the particles rather than slowing them down.

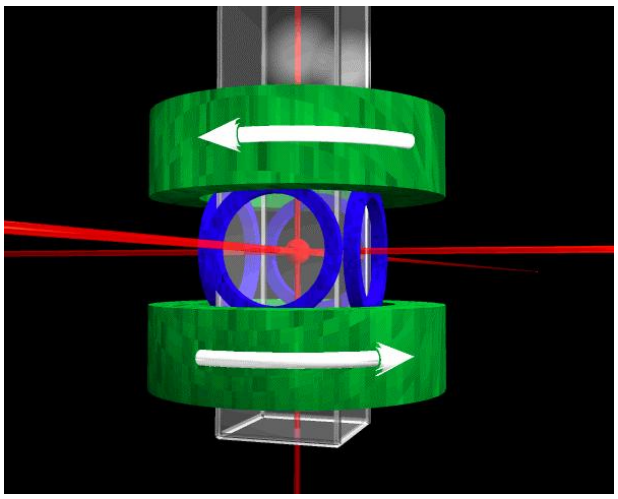


Figure 7 – Schematic representation of the experimental setup developed by Wieman's group. Note that the laser beams all converge to the center of the trap, playing the role of cooling the sample. The white arrows indicate the time orbiting potential, responsible for maintaining the particles in the same spin state [8]. Figure taken from Ref. 38.

Evaporative cooling on the other hand is favoured at high densities [28]. Cornell and co-workers built an apparatus that combined both cooling methods. Initially, the particles were trapped by an MOT and thus laser-cooled to the point at which the system's density became ideal to evaporative cooling. Then, the laser beams are turned off and the Time orbiting potential trap is turned on (TOP). This new trapp was developed with the goal of avoiding the so-called Majorana flips which represented a limitation of the MOTs [39].

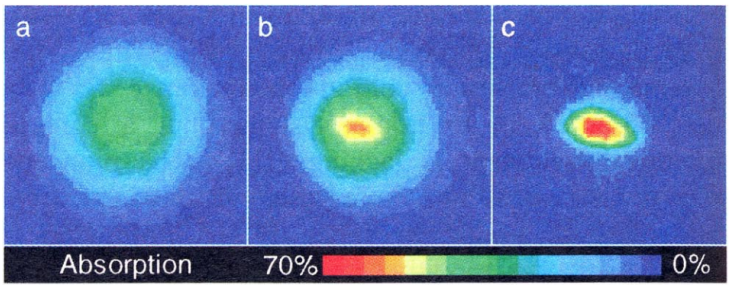


Figure 8 – Velocity distribution of sodium atoms in the vapor utilized by Ketterle's group. A beam of light was emitted in the sample and the shadow it cast provided data about the velocities of the particles. (a) displays a gas cloud just above the condensation temperature while (b) shows that a few particles are already condensed and (c) displays the system in temperatures way below the condensation temperature. Note that the ellipsoidal shape of the gas cloud is also present in these results [9]. Figure taken from Ref. [9].

These flips are a consequence of the fact that the laser responsible for trapping the atoms in the MOTs cancels each other at the center of the trap, allowing certain spin fluctuations [9]. The setup developed by Cornell consisted of a rotational magnetic field that covered the entire area of the trap thus preventing such phenomena [40]. The first signs of condensation appeared at temperatures of 170 nK with a number of particles in the order of 2×10^4. When such temperatures were reached, the TOP was turned off for a certain amount of time in order to allow the atomic vapor to disperse. During this process, a beam of light was cast on the vapor, and by analyzing the shadow of the sample cast, it was possible to confirm the manifestation of a BEC. The regions that cast a stronger shadow, are at the center of the cloud, i.e., the region that contains the colder/slower atoms while the surrounding regions contain the faster atoms that were escaping the trap. The velocity distribution was such that the non-condensed atoms, i.e., the atoms that were further away from the center of the trap, presented an isotropic and regular velocity distribution, which is an expected result for gases in thermal equilibrium [14]. Such behavior is displayed at insert A in Fig. 9. The atoms at the center of the trap, however, presented an anisotropic velocity distribution which is a reflection of the irregularities of a TOP. The fact that a whole portion of the cloud obeyed an anisotropic velocity distribution, was a strong indication that all those particles were governed by the same wave function, one of the main features of a Bose-Einstein condensate. Such a statement is reasonable because the extremely low temperatures implicated that such particles had practically zero thermal energy so the only energy scale present was from the TOP. The ellipsoidal shape displayed at inserts B and C in Fig. 9 is a direct manifestation of the non-uniform velocity distribution of the particles at the center of the trap. Interestingly, Wieman's group was not the only one making efforts to achieve a BEC at the time. Wolfgang Ketterle's group at MIT was also into it and they succeded as well using sodium instead of rubidium as the sample [9]. The condensation started to take place at temperatures of the order of $\sim 2\mu$K and the

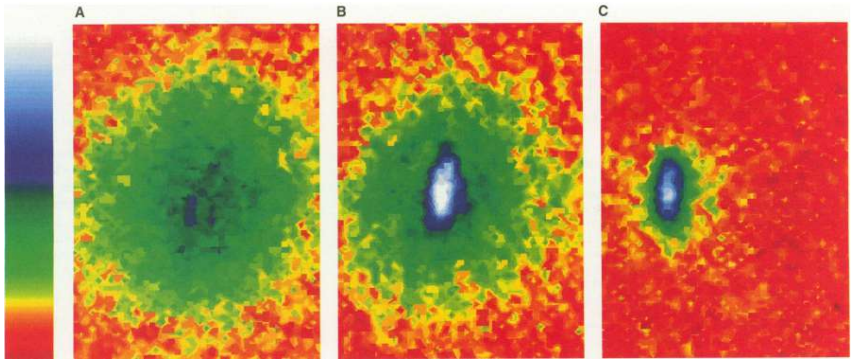


Figure 9 – Velocity distribution of the particles. The darker regions in the center of the figure represent the colder and slower atoms that remained trapped after evaporative cooling took place. Insert (A) showcases the system at temperatures above T_c, (B) shows the moment the condensation starts to take place at temperatures $\sim T_c$ and in (C) we can see the ellipsoidal shape of condensed particles. Figure taken from Ref. [8].

results achieved by them are very similar to the ones mentioned before, see in Fig. 8. For their outstanding achievements in experimental Physics, Wieman, Cornell, and Ketterle shared the Nobel Prize in Physics in 2001.

4.4 THE SOLID STATE PHYSICS LABORATORY

The experiments performed under the supervision of Prof. Dr. Mariano de Souza at the *Solid State Physics Laboratory* at Unesp Rio Claro, lay the foundation for all the results obtained by the research group, both theoretical and experimental ones. Most importantly, measurements of the thermal expansion coefficient and dielectric constant at low temperatures in systems such as the Fabre-Bechgaard salts are carried in a cryostat of the model Teslatron PT, provided by Oxford Instruments, with financial support by Fapesp (Grants-2011/22050-4). The mentioned class of materials is interesting because they present a rich phase diagram, which includes a superconducting phase [41]. Hence, by controlling parameters such as pressure and temperature, it becomes possible to experimentally access phase transitions and critical phenomena. Interestingly, measurements of the thermal expansion (α_p) coefficient are of extreme importance in this context. As we have already mentioned before, can be used to track and evaluate phase transitions and critical phenomena. Recalling that α_p is incorporated in the definition of the Grüneisen ratio and it is responsible for the singular behavior of Γ on the verge of critical points [19], it becomes possible to experimentally access the singular behavior of Γ. Hence, theory and experiment supplement each other, providing precise and concise results. Furthermore, α_P can be written in terms of the derivative of the Helmholtz free energy with respect to volume and temperature. Hence, by measuring the thermal expansion coefficient, it becomes possible to experimentally access in an indirect way the system's free energy. The measurements of the thermal expansion coefficient are made by means of an analysis of the changes in capacitance between the two plates of a dilatometric cell.

*Thanks to Fapesp, Grants - 2011/22050-4



Figure 10 – The Solid State Physics Laboratory in Rio Claro, SP at São Paulo State University

The material which is being analyzed is fixed to one of the plates of the capacitor. Such a plate is mobile and, as the solid expands, the distance between the plates decreases and thus the capacitance between them is increased. By recording the values of capacitance, it is possible to infer how much the solid expanded, and thus the thermal expansion coefficient can be computed. Interestingly, measurements of α_p can provide more information than one can usually expect. Besides telling us how the dimensions of a sample change with temperature, we can also experimentally verify the theoretical results predicted under the light of Γ [10]. The functioning of the Teslatron PT cryostat consists essentially of a closed cycle of He^4 which is cooled by a compressor. The He^4 gas goes through the lines and can cool the system down to temperatures in the order of 1.4 K. The pressure in the circulating lines is controlled by the so-called needle valve. Thus, by controlling temperature and pressure it is possible to access various exotic phases of matter. In order to maintain optimal conditions for the system to cool down, the lines at which He^4 circulates need to be cleaned from time to time. Such a procedure is executed with vacuum pumps, which purge the circulation lines and thus remove any moisture that could compromise the experiments. Additionally, we have the so-called zeolite trap, which is responsible for retaining impurities present in the gas. By means of the vacuum pumps and the zeolite trap, optimal conditions for the realization of the experiments are ensured. Considering the points discussed, it becomes clear that although BEC experiments are not performed at the *Solid State Physics Lab*, the performed experiments are of vital importance in understanding theoretical results. In the following, we shall discuss the basic aspects concerning the system cool-down, covering the most important steps in order to achieve temperatures in the scale of 1.4 K. First, we confine approximately 0.6 bar of the circulating gas in a storage tank. In order to guarantee homogeneity of the circulation of the gas in the lines, which is crucial for the achievement of low temperatures, the tank is open and the gas is left circulating for around 12 hours before the cooldown is actually started. Next, the F-70 Sumitomo compressor is turned on, which is responsible for cooling the circulating gas. To avoid an overheating of the compressor, the system is connected to a refrigerating device known as a chiller. Such equipment is responsible for continuously cooling the compressor through a flow of water at approximately 17.5°C. With that in mind, the chiller must be turned on around 15 minutes before the compressor.

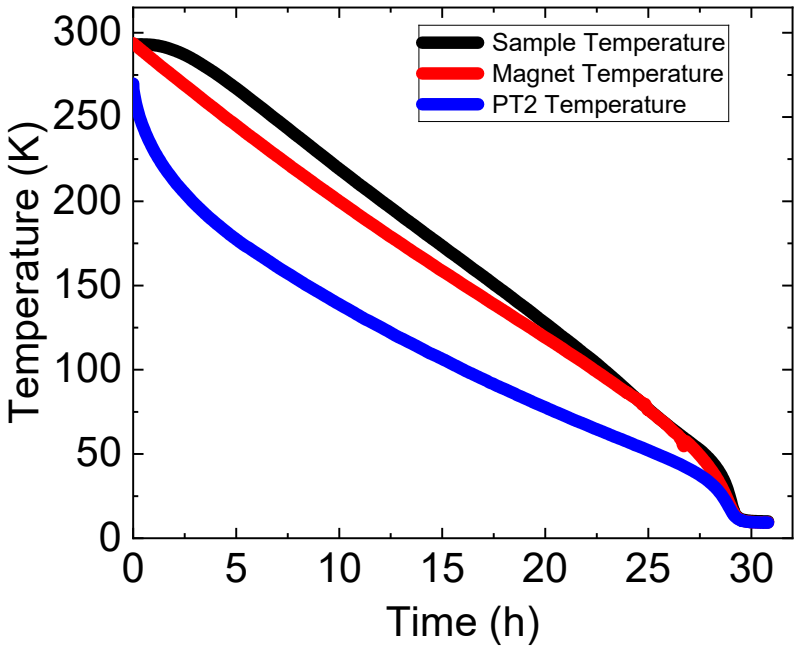


Figure 11 – Typical profile of the PT2, magnet, and sample space temperatures as a function of time. We can see that the PT2 temperature is diminished at a faster rate, that is because it is in direct contact with the circulating gas.

The main goal of performing such previously discussed procedures is to cool down the sample space, where the sample rod is inserted. The sample rod is the equipment to which the material under analysis is attached. Such low temperatures are achieved in the sample space through its contact with other parts of the cryostat which are cooled before. The circulating gas is in fact in contact with the so-called PT2 which in turn is in contact with the magnet located in the basis of the cryostat. The magnet exchanges heat with the sample space through an exchange gas in its interior. Hence, it is expected that the PT2 is cooled at a faster rate, followed by the magnet, and thus the sample space. The measurements of the temperatures of these three components of the cryostat are collected through a routine in software installed in the computer. Fig. 11 displays the values of temperature for the PT2, the magnet, and the sample space as a function of time. Heat exchanges between the sample space and its surroundings is prevented due to the outer vacuum chamber (OVC) which isolates the sample space. The cooldown at which these curves were observed, was performed in the context of the measurements of the thermal expansion coefficient of the material known as purple bronze. The experiment occurred in the first week of August of 2024 and was supervised by Prof. Dr. Mariano de Souza and with the support of post-doc Lucas Squillante. Other students of Prof. Dr. Mariano and I had the opportunity to accompany and assist in the realization of the experiments.

5 EXPLORING THE THERMODYNAMICS OF THE NON-IDEAL BEC

The goal of this chapter is to estimate and analyze the behavior of the Grüneisen parameter on the verge of the BEC of interacting particles. To do so, we shall rely on seminal books of Statistical Mechanics and thermodynamics and also, on results reported in the literature. Recently, parameters that emulate the role played by pressure and volume in harmonic trapped gas were defined in order to make the thermodynamic analysis of such systems possible. Hence, by collecting experimental data reported in the literature concerning the measurements of such parameters, we shall obtain and analyze both α_P and c_P and naturally Γ. We shall discuss the behavior of α_P and c_P near T_c.

5.1 VOLUME AND PRESSURE PARAMETERS FOR HARMONICALLY TRAPPED PARTICLES

As we have already discussed, harmonic traps are essential for the experimental realization of the Bose-Einstein condensation [8, 9]. The efficiency and physical accuracy of the framework associated with harmonic trapped BECs are well established in the literature. However, the thermodynamic analysis of a harmonic-trapped BEC still remained a topic of discussion. This is due to the particles being imprisoned by a three-dimensional external harmonic potential U_{ext}, given by [16]:

$$U_{ext} = \frac{1}{2} m \left(\omega_x^2 x^2 + \omega_y^2 y^2 + \omega_z^2 z^2 \right), \tag{5.1}$$

where ω_i are oscilation frequencies in each direction and x, y, z the spatial coordiantes [16]. The fact that the particles are imprisoned by a potential and not by rigid walls implies that the quantity known as volume, loses its meaning. Additionally, due to the absence of walls, the concept of pressure, defined as the force applied to a certain area, also loses its meaning because there is no area where the force can be applied. Since such fundamental properties as volume and pressure are not applicable in this scenario, the thermodynamic analysis of this sort of system is jeopardized. In this context, it was recently proposed that such analysis could be evaluated under the light of newly introduced thermodynamic parameters which would emulate well-known quantities like volume and pressure [16]. Such parameters are defined as:

$$\mathcal{V} = \frac{1}{\omega_x \omega_y \omega_z}; \quad \mathcal{P} = \frac{2}{3} \omega_i^3 \langle U_{ext} \rangle . \tag{5.2}$$

The physical interpretation of the so-called volume parameter $\mathcal{V}$ can be facilitated if we recall the connection between frequency and energy. Since ω_i denotes the frequency of oscillation of the confining potential, we can infer that high values of ω_i implicate in a large value of energy associated with the potential.

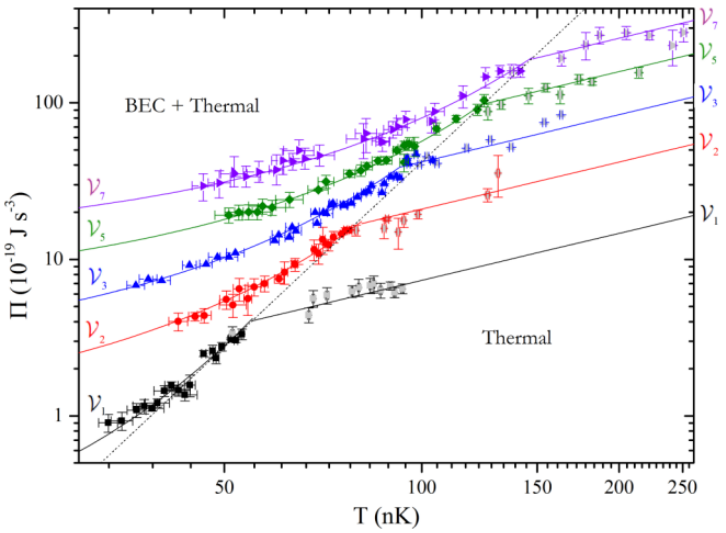


Figure 12 – Pressure parameter Π at constant volume parameter as a function of the temperature. The regions indicated by *BEC* and *BEC+Thermal* refer to conditions in which the system is mixed, presenting a condensed phase and a gaseous and also where the gaseous phase is dominant respectively. The values of constant volume parameter are $\mathcal{V}_1 = (1.9 \times 10^{-7})\text{s}^3$, $\mathcal{V}_2 = (6.4 \times 10^{-7})\text{s}^3$, $\mathcal{V}_3 = (3.2 \times 10^{-7})\text{s}^3$, $\mathcal{V}_5 = (1.75 \times 10^{-7})\text{s}^3$, $\mathcal{V}_7 = (1 \times 10^{-7})\text{s}^3$. Figure taken from Ref. [42].

Hence, the mobility of the particles in the energy levels of such potential is restricted. That is because a very small number of particles have the necessary energy to transit through the higher energy levels. Thus, high frequencies characterize a small volume parameter. On the other hand, for a potential that oscillates with lower frequencies, the energy associated to it would be also small. Under these conditions, the mobility of the particles through the energy levels is enhanced. Thus, smaller frequencies characterize a large volume parameter. The pressure parameter is interpreted as the manner in which the potential is distributed along the possible values of ω, i.e., how it is distributed along the volume parameter. This interpretation is reminiscent of the ideal gas law, written in the form $P = \frac{2}{3}U/v$, where U is the internal energy of the gas. Recently, measurements of such parameters as a function of temperature and as a function of one and other were reported for a system composed of 10^5 Rb atoms [42, 43]. Fig. 12 showcases the pressure parameter as a function of the temperature. Note that above the critical temperature, we observe that $\mathcal{P}$ grows linearly with T in a behavior typically associated with the ideal gas. This is due to the fact that for high temperatures, the equation of state of the boson gas becomes simply the ideal gas law [14]. For temperatures bellow T_c, $\mathcal{P}$ assumes a different dependence with T. This change is due to the fact that at low temperatures, quantum effects become more expressive and we observe a deviation from the classical case. We can compare the results shown in Fig. 12, which were extracted from Ref. [42] with the equation for the state of the ideal Bose gas. Figure 13 displays the equation of state of the Fermi, and Bose gas and also of the classical ideal gas. Also Fig 13 indicates the occurrence of the formation of the Bose-Einstein condensate and the Fermi liquid regime.

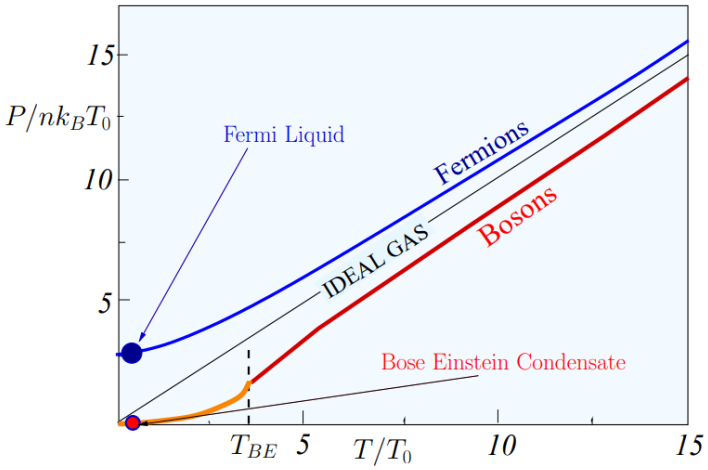


Figure 13 – Comparison between the equations of state of the ideal classical gas and ideal quantum gases as a function of the relative temperature $\frac{T}{T_0}$ where T_0 is a reference value of T. Note that at high temperatures the two quantum gases behave essentially as a classical ideal gas. For low temperatures, quantum effects need to be taken into account and thus each gas behaves in a unique manner. The formation of the Bose-Einstein condensate and the Fermi liquid is indicated at $T = 0$. Figure taken from Ref. [29].

We can see that at high temperatures the two quantum gases behave like a classical ideal gas. At low temperatures, the two types of gases behave distinctly and that is because at low temperatures, quantum effects become expressive. As a consequence of Pauli's exclusion principle, for $T \to 0$, the particles of the Fermi gas distribute along a number of energy levels. The highest energy level occupied is the Fermi level, with an Fermi energy ε_f associated with it [5]. Hence, the pressure of the Fermi gas at $T = 0$ is due to the finite energy scale associated with the Fermi level, which remains at $T = 0$. On the other hand, the Bose gas goes through the Bose-Einstein condensation as discussed above. The ground state energy of an ideal Bose gas is given by:

$$\varepsilon_1 = \frac{3h^2}{8m}\frac{1}{V^{2/3}}. \tag{5.3}$$

The value of this number is of the order of 10^{-18} eV, [5]. These value was obtained considering the mass of one helium atom and $v = 10^{-6}m^3$ Thus, it is common to approximate the energy of the ground state of the ideal Bose gas to zero. Since all particles condense into the ground state, i.e., $\varepsilon = 0$, the pressure naturally becomes null. Figure 14, depicts the volume parameter as a function of temperature. Just as with the conventional volume, the volume parameter also increases with temperature. In the context of harmonic trapped particles, the volume parameter increases with temperature because thermal energy is being added to the system, thus permitting the particles to occupy higher energy levels. In the same manner as the pressure parameter, for $T > T_c$ the volume grows linearly with temperature, following the ideal gas law, while for $T < T_c$, quantum effects cause

the dependence between $\mathcal{V}$ and T to change. [43]. From the isochore curves in Fig. 12 the authors of Ref. [42] were able to plot the isotherms for this system which are displayed at Fig. 15. The behavior of the $\mathcal{V}$ vs $\mathcal{P}$ curves follows the same pattern as the other plots, with the condensation causing a change in the dependence between $\mathcal{V}$ and $\mathcal{P}$. Curiously, in the mixed regime, $\mathcal{V}$ and $\mathcal{P}$ still depend on each other, while in the ideal case, the volume becomes pressure-independent [14]. With these three plots we just discussed, we will be able to access the thermodynamic quantities required to evaluate Γ.

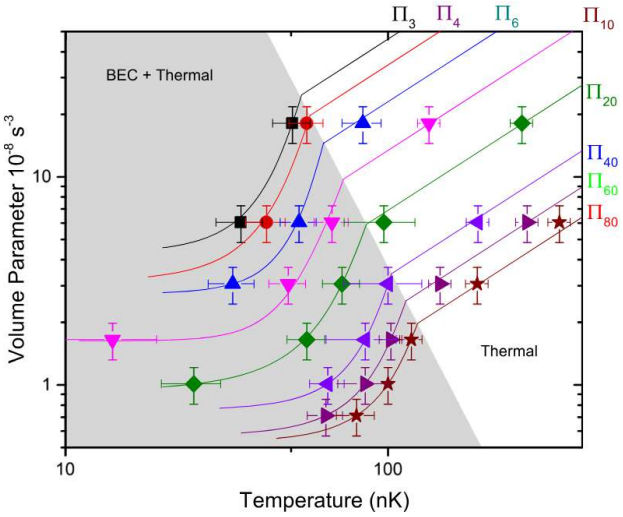


Figure 14 – Volume parameter at constant pressure parameter as a function of temperature. The grey region indicated by *BEC+Thermal* corresponds to conditions where the system presents a mixture of condensed and uncondensed particles. The white region indicated by *Thermal* corresponds to conditions where the gaseous phase is dominant. In the same manner as in Fig. 12, the change in the dependence on temperature is a consequence of the Bose-Einstein condensation. The various different values of pressure parameter are $\mathcal{P}_3 = (3 \times 10^{-19})\text{J s}^3$, $\mathcal{P}_4 = (4 \times 10^{-19})\text{J s}^3$, $\mathcal{P}_6 = (6\times10^{-19})\text{J s}^3$, $\mathcal{P}_{10} = (10\times10^{-19})\text{J s}^3$, $\mathcal{P}_{20} = (20\times10^{-19})\text{J s}^3$, $\mathcal{P}_{40} = (40\times10^{-19})\text{J s}^3$, $\mathcal{P}_{60} = (60 \times 10^{-19})\text{J s}^3$, $\mathcal{P}_{80} = (80 \times 10^{-19})\text{J s}^3$. Figure taken from Ref. [43].

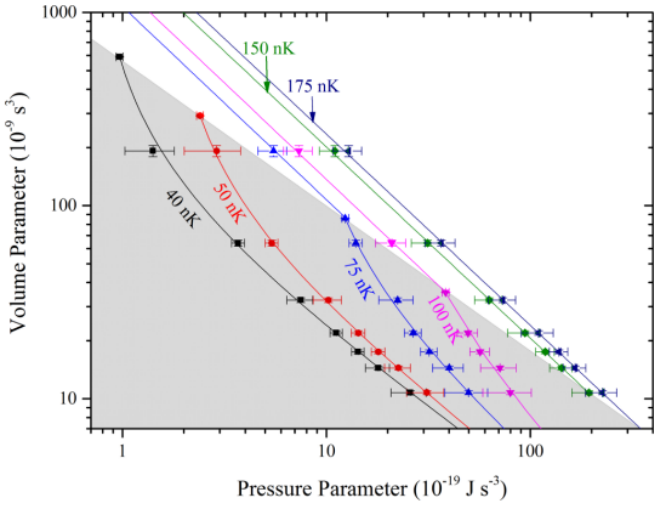


Figure 15 – Volume parameter as a function of the pressure parameter at constant temperature, i.e., the isotherms of an interacting Bose gas. The labels *BEC+Thermal* in the grey region and *Thermal* in the white one follow the pattern of Fig. 14. The various temperature values are indicated in the graph. Figure taken from Ref. [42].

5.2 COMPUTING THE GRÜNEISEN RATIO

As we have already discussed, Γ is defined as the ratio between the thermal expansion coefficient and the specific heat, both at constant pressure. In this section, we shall plot Γ for harmonic trapped interacting particles. Naturally, the thermal expansion and specific heat will be expressed in terms of the volume $\mathcal{V}$ and pressure $\mathcal{P}$ parameters instead of the conventional volume and pressure. Hence, we shall denote such quantities for harmonic trapped particles as $\alpha_{\mathcal{P}}$ and $c_{\mathcal{P}}$. We shall begin with the specific heat at constant pressure parameter, which we can obtain through the relation we derived in earlier sections:

$$c_{\mathcal{P}} = c_{\mathcal{V}} - T\frac{\left(\frac{\partial \mathcal{P}}{\partial T}\right)^2_{\mathcal{V}}}{\left(\frac{\partial \mathcal{P}}{\partial \mathcal{V}}\right)_T}. \tag{5.4}$$

In Ref. [44], $c_{\mathcal{V}}$ is given by:

$$c_{\mathcal{V}} = \frac{3}{\omega_i^3}\left(\frac{\partial \mathcal{P}}{\partial T}\right)_{\mathcal{V}}. \tag{5.5}$$

With the plots shown in the last section, we can extract the required derivatives and plot $c_{\mathcal{P}}$. Due to the small number of experimental points, we considered also the points associated to the fittings. In Fig. 16 we can see the specific heat at constant pressure parameter as a function of the temperature. For values of T near T_c we can see that $c_{\mathcal{P}}$ is enhanced and to understand the reasons behind such enhancement, we must recall the connection between $c_{\mathcal{P}}$, the entropy, and the ground state energy. As we decrease the temperature to values below T_c, the particles begin to condense in the system's ground state. The energy scale of such a state is independent of T and thus does not contribute to the system's entropy [14]. Hence, in the limit of $T \to 0$, all the particles will occupy the ground state and thus $S \to 0$. Since $c_{\mathcal{P}}$ can be written in terms of the derivative of S

with respect to T, when $S = 0$ the specific heat will also go to zero. With that in mind, if we increase the temperature from values below T_c, the particles will start to occupy the excited states, which contribute to the system's entropy. Due to this enhancement in entropy, an enhancement in the specific heat is also observed. In Ref. [44], $c_{\mathcal{V}}$ was computed and also exhibited an enhancement for $T \simeq T_c$. Now we shall analyze $\alpha_{\mathcal{P}}$ on the verge of the BEC. From Fig. 14, we extract the derivative of the volume parameter with respect to T and by comparing the values of such derivative with a reference volume parameter $\mathcal{V}_0$, the thermal expansion coefficient is plotted. We can observe that $\alpha_{\mathcal{P}}$ also increases for $T \simeq T_c$, though in a more intense manner. Such behavior is in accordance with the results concerning measurements of $\alpha_{\mathcal{P}}$ in Ref. [43].

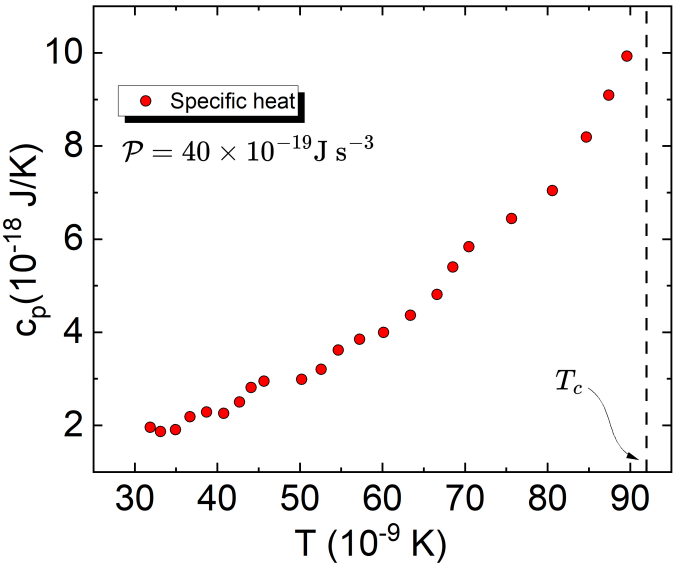


Figure 16 – Specific heat at constant pressure parameter for 10^5 harmonic trapped Rb atoms. The increase in the value of $c_{\mathcal{P}}$ is associated with an increase in entropy. The constant value of pressure is indicated as well as the approximate value of the critical temperature $T_c \simeq 92$ nK.

In fact, $\alpha_{\mathcal{P}}$ also depends on the entropy but such dependence is different from the one presented by $c_{\mathcal{P}}$ [13]. We can access this information if we write both quantities in terms of the free energies. It is possible to write $c_{\mathcal{P}}$ in terms of the Gibbs free energy following the discussion in chapter 2. The thermal expansion coefficient can be expressed in terms of the Helmholtz free energy [13]:

$$\alpha_{\mathcal{P}} = \frac{1}{\mathcal{V}_0}\left(\frac{\partial \mathcal{V}}{\partial T}\right)_{\mathcal{P}} = -\frac{1}{\mathcal{V}_0}\left(\frac{\partial \mathcal{V}}{\partial P}\right)_{T}\left(\frac{\partial S}{\partial \mathcal{V}}\right)_{T} \tag{5.6}$$

$$\alpha_{\mathcal{P}} = \kappa_T\left(\frac{\partial S}{\partial \mathcal{V}}\right)_{T} = \kappa_T\left(\frac{\partial \mathcal{P}}{\partial T}\right)_{\mathcal{V}} = -\kappa_T\left(\frac{\partial^2 F}{\partial \mathcal{V}\partial T}\right). \tag{5.7}$$

In the derivation above, we made use of the relation $\left(\frac{\partial \mathcal{V}}{\partial T}\right)_{\mathcal{P}} = -\left(\frac{\partial \mathcal{V}}{\partial P}\right)_{T}\left(\frac{\partial S}{\partial \mathcal{V}}\right)_{T}$ and also of the Maxwell relation $(\partial S/\partial \mathcal{V})_T = (\partial \mathcal{P}/\partial T)_{\mathcal{V}}$ [13]. By writing the expressions for both $c_{\mathcal{P}}$ and $\alpha_{\mathcal{P}}$ side by side we have:

$$c_{\mathcal{P}} = -T\left(\frac{\partial^2 G}{\partial T^2}\right)_{p}; \quad \alpha_{\mathcal{P}} = -\kappa_T\left(\frac{\partial^2 F}{\partial \mathcal{V}\partial T}\right). \tag{5.8}$$

Note that $c_{\mathcal{P}}$ only incorporates variations of the G with respect only to temperature. On the other hand, $\alpha_{\mathcal{P}}$ incorporates the variations of F with respect to not only temperature but also pressure. Hence, the entropy associated to F in $\alpha_{\mathcal{P}}$ is sensible to changes in T and in $\mathcal{V}$. For $c_{\mathcal{P}}$, the entropy only is affected by the temperature.

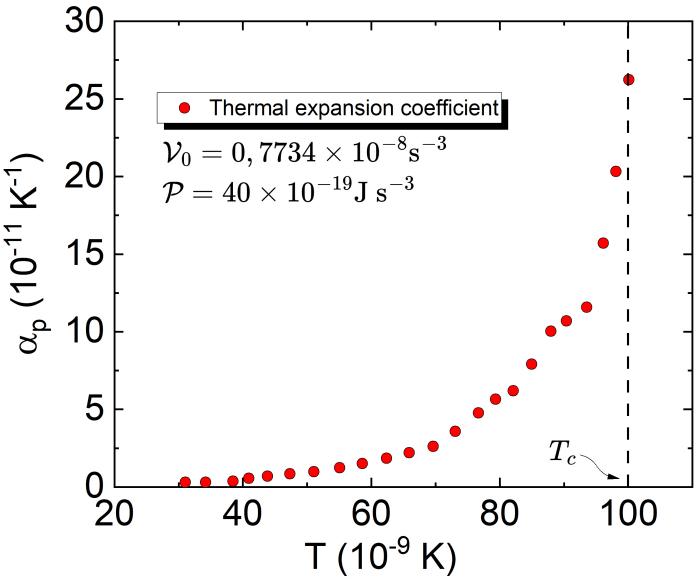


Figure 17 – Thermal expansion coefficient at constant pressure parameter as a function of temperature. We can see that $\alpha_{\mathcal{P}}$ is dramatically enhanced for temperatures near T_c, more details in the main text. The constant pressure parameter value is indicated in the figure as well as the approximate value of the critical temperature $T_c \simeq 100$ nK.

Hence, the interplay between the free energy and quantities like $\mathcal{V}$ and T is what dictates the entropy sensibility to external stimuli. Due to this high sensitivity to changes in entropy, $\alpha_{\mathcal{P}}$ and naturally Γ were identified as the singular part of Γ_{eff} [19, 45]. With both $\alpha_{\mathcal{P}}$ and $c_{\mathcal{P}}$ in hands, it became possible to plot Γ as a function of T. As expected, the expressive enhancement in $\alpha_{\mathcal{P}}$ was carried to Γ as we can see in Fig. 18. This behavior of Γ is a fingerprint of various phase transitions and critical phenomena [10, 46]. It is worth mentioning that Γ was computed for the ideal BEC in a publication of our research group [12]. In the following, a comparison between the results obtained in this project and the ones reported in Ref. [12] will be made. In this context, Γ was computed via the relation:

$$\Gamma = v\frac{(\partial p/\partial T)}{\partial E/\partial T}_{v}. \tag{5.9}$$

Note that the denominator is simply the specific heat at constant volume c_v [12]. According to Ref. [47], the pressure derivative with respect to the temperature of an ideal Bose gas, below its critical temperature is:

$$\frac{\partial p}{\partial T} = \frac{\partial}{\partial T}\left[0.0851 m^{3/2}(k_B T)^{5/2}\hbar^{-3} g\right] = 0.21275 m^{3/2}(k_B T)^{3/2} k_B \hbar^{-3} g \tag{5.10}$$

where g is the degeneracy.

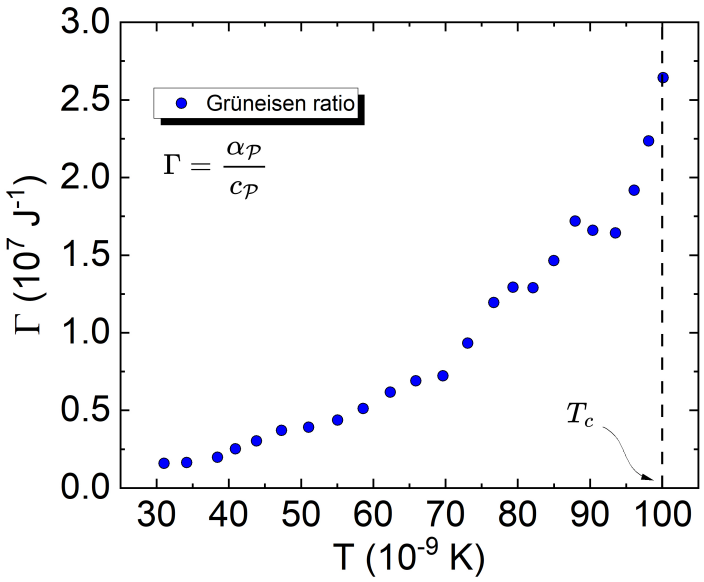


Figure 18 – $\alpha_{\mathcal{P}}$ as a function of T. We can see that $\alpha_{\mathcal{P}}$ is dramatically enhanced for temperatures near T_c, more details in the main text. The constant pressure parameter value is indicated.

Additionally, we have that c_v for the ideal Bose gas below the critical temperature is:

$$c_v = 1.926 N k_B \left(\frac{T}{T_c}\right)^{3/2}. \tag{5.11}$$

The ratio between Eqs. 5.10 and 5.11 was evaluated and thus it was achieved that for an ideal Bose gas, Γ is constant. That is because the $T^{3/2}$ crosses out. Hence, we can note the difference between the behavior of Γ for the ideal BEC and its non-ideal counterpart. For the non-interacting case, the system behaves similarly as the classical ideal gas, presenting a constant Γ [12]. For the interacting case, the non-ideality of the system causes Γ to scale with the temperature in a non-linear form as we can see in Fig. 18.

6 CONCLUSIONS AND PERSPECTIVES

In this B. Sc. work, a general overview of the BEC was presented. Starting from a review of Statistical Mechanics and Thermodynamics, we covered fundamental aspects concerning phase transitions, critical phenomena, and the ideal BEC. Furthermore, a discussion about the effects of interactions was made in which the framework of the weakly interacting Bose gas was unraveled in a step-by-step manner. In this same section, insights concerning the effects of interaction were pointed out, under the light of recent results concerning the Brillouin paramagnet. Experimental and historical aspects were also reviewed in chronological order, starting from the theoretical proposal by Einstein and Bose to the experimental realizations in 1995. The pivotal importance of the experiments conducted in the *Solid State Physics lab* under the guidance of Prof. Dr. Mariano de Souza was discussed. An overview of how to reach low temperatures was presented, as well as a discussion concerning the valuable information we can extract from thermal expansion measurement experiments. Finally, a thermodynamic analysis of the non-ideal BEC was made in terms of the volume and pressure parameters and the Grüneisen ratio. In such analysis, we discussed the behavior of quantities like the thermal expansion coefficient and specific heat on the verge of condensation. We computed the Grüneisen ratio and compared the results achieved in this work with results reported in the literature concerning the ideal condensation. The behavior presented by the analyzed quantities was consistent with consolidated works in the literature.

BIBLIOGRAPHY

R. Baierlein, *Thermal Physics*, 1st ed. (Cambridge University Press 1999).

A. Einstein, Sitzber. Kgl. Preuss. Akad. Wiss. **8**, 3-14 (1925).

S. Bose, Z. Physik **26**, 178 (1924).

M. H. Anderson, J. R. Mansher, M. R. Matthews, C. E. Wieman, E. A. Cornell, Science **269**, 198 (1995).

K. B. Davis, M. O. Mewes, M. R. Andrews, N. J. van Druten, D. S. Durfee, D. M. Kurn, W. Ketterle, Phys. Rev. Lett. **75**, 22 (1995).

I. F. Mello, L. Squillante, G. O. Gomes, A. C. Seridonio, M. de Souza, J. Appl. Phys. **128**, 225102 (2020).

L. Squillante, I. F. Mello, G. O. Gomes, A. C. Seridonio, R. E. Lagos-Mônaco, H. E. Stanley, M. de Souza, Sci Rep **10**, 7981 (2020).

M. de Souza, P. Menegasso, R. Paupitz, A. C. Seridonio, R. E. Lagos-Mônaco, Eur. J. Phys **37**, 055105 (2016).

H. E. Stanley, *Introduction to Phase Transition and Critical Phenomena* 1st ed. (Oxford University Press, New York, 1971).

R. K. Pathria, *Statistical Mechanics* 2nd ed. (Elsevier Butterworth Heinemann 1996).

E. M. Lifshitz, L. Pitaevskii, *Course of Theoretical Physics vol 9*, 2nd ed. (Butterworth-Heinemann 1980).

V. Romero-Rochín, Phys. Rev. Lett. **94**, 130601 (2005).

H. B. Callen *Thermodynamics and an Introduction to Thermostatistics*, 2nd ed. (Wiley 1991).

E. Grüneisen, Annalen der Physik **344**, 257-306 (1912).

L. Zhu, M. Garst, A. Rosch, Qimiao Si, Phys. Rev. Lett. **91**, 066404 (2003).

L. Squillante, I. F. Mello, A. C. Seridonio, M. de Souza, J. Appl. Phys. **142**, 111413 (2011).

L. D. Landau, E. M. Lifshitz, *Course of Theoretical Physics vol 3*, 3rd ed. (Butterworth-Heinemann 1981).

L. D. Landau, E. M. Lifshitz, *Course of Theoretical Physics vol 5*, 2nd ed. (Pergamon, Press London-Paris 1959).

C. Cohen-Tannoudji, B. Diu, F. Laloe, *Quantum Mechanics, vol. 1* 1st ed. (Wiley 1971).

E. Butkov *Mathematical Physics*, 1st ed. (Addison-Wesley 1968).

G. B. Arfken, H. J. Webber, F. E. Harris *Mathematical Methods for Physicists: A Comprehensive Guide*, 7th ed. (Academic Press 2012).

H. Goldstein, C. Poole, J. Safko *Classical Mechanics*, 3rd ed. (Pearson 2001).

C. Cohen-Tannoudji, B. Diu, F. Laloe, *Quantum Mechanics, vol. 3*, 1st ed. (Wiley 2020).

W. Ketterle, N. J. van Druten, *Advances in Atomic, Molecular, and Optical Physics* (1996).

P. Coleman, *Introduction to Many-Body Physics*, 1st ed. (Cambridge University Press 2016).

N. Bigagli, W. Yuan, S. Zhang, B. Bulatovic, T. Karman, I. Stevenson, S. Will, Nature **631**, 289-293 (2024).

F. London, Nature **141**, 643-644 (1938).

J. Wilks, D. S. Betts, *Introduction to Liquid Helium* 2nd ed. (Oxford University Press, 1987).

V. S. Letokhov , J.of Exp. Theor. Phys. Lett. **7**, 272 (1968).

T. W. Hansch, A. L. Schawlow, *Cooling of gases by laser radiation* (Opt. Commun. 1992).

P. D. Lett, R. N. Watts, C. I. Westbrook, W. D. Phillips, P. L. Gould, H. J. Metcalf, Phys. Rev. Lett. **61**, 169 (1988).

E. L. Raab, M. Prentiss, A. Cable, S. Chu, D. E. Pritchard, Phys. Rev. Lett. **59**, 2631 (1987).

I. F. Silveira, M. Reynolds, J. Low. Temp. Phys **87**, 343 (1992).

P. W. Anderson, Phys. Rev. **130**, 439 (1963).

D. M. Brink, C. V. Sukumar, Phys. Rev. A. **74**, 035401 (2006).

W. Petrich, M. H. Anderson, J. R. Ensher, E. A. Cornell, Phys. Rev. Lett. **74**, 3352 (1995).

A. C. Jacko, H. Feldner, E. Rose, F. Lissner, M. Dressel, Roser Valentí, H. O. Jeschke Phys. Rev. B. **87**, 155139 (2013).

F. J. Poveda-Cuevas, P. Castilho, E. D. Mercado-Gutierrez, A. R. Fritsch, S. R. Muniz, E. Lucioni, G. Roati, V.S. Bagnato, Phys. Rev. A **92**, 013638 (2015).

E .D. Mercado Guitérrez, F. J. Poveda-Cuevas, V.S. Bagnato, Brazilian J. of Phys. **48**, 539-542 (2018).

R. F. Shiozaki, G. D. Telles, P. Castilho, F. J. Poveda-Cuevas, S. R. Muniz, G. Roati, V. Romero-Rochín, V.S. Bagnato, Phys. Rev. A **90**, 043640 (2014).

L. Bartosch, M. de Souza, M. Lang, Phys. Rev. Lett. **104**, 254701 (2010).

L. Squillante, L. S. Ricco, A. M. Ukpong, A. C. Seridonio, R. E. Lagos-Mônaco, M. de Sozua, Phys. Rev. B **108**, 140403 (2023).

A. L. Feller, J. D. Walecka, *Quantum Theory of Many-Particle Systems*, 1st ed. (New York: Dover 2003).